ANALYSIS OF PERMANENT MAGNET SYNCHRONOUS MOTOR DRIVE

A DISSERTATION

Submitted in partial fulfilment of the
requirements for the award of the degree
of
MASTER OF ENGINEERING
in
ELECTRICAL ENGINEERING
(With Specialization in Power Apparatus and Electric Drives)

SATYA PRAKASH DUBEY

DEPARTMENT OF ELECTRICAL ENGINEERING
UNIVERSITY OF ROORKEE
ROORKEE–247 667 (INDIA)

JANUARY, 2000

ACKNOWLEDGEMENT

I wish to place on record my deep sense of gratitude and indebtedness to my guide **Dr. S.P. Srivastava**, Associate Professor, Department Of Electrical Engineering, University Of Roorkee, Roorkee. I am grateful for the long hours they spend in discussing and explaining minute details of the work. I consider myself privileged to have worked under his supervision and guidance.

I am highly thankful to Shri Y.P. Singh, O.C. Drives Lab. Electrical Engineering Department , University of Roorkee, Roorkee; for providing Laboratory facilities.

I am grateful to all my teachers of Drives group of their suggestions and constant encouragement.

Grateful acknowledgements are also due to all my friends and well wishers whose timely help has gone a long way in this dissertation work.

(SATYA PRAKASH DUBEY)

ABSTRACT

The growing interest in energy saving especially in industrial applications has led to explore in more details the potential of unconventional excitation system for electric machines. The PM motor has the potential to replace the induction and wound field commutator motor in a number of industrial, commercial and domestic variable speed drive are based largely on its energy saving capability. The use of the permanent magnet in the rotor of the PM motor makes it unnecessary to supply magnetizing current through the stator for constant air gap flux. The stator current needs to be only torque producing. Hence for the same output the PM motor will operate at higher power factor and will be more efficient than conventional motors.

The dynamic performance of permanent magnet synchronous motor (PMSM) drive fed through a current hysteresis controlled voltage source inverter (VSI) is investigated. First, the mathematical modeling of machine and control assembly is described, then a numerical simulation of this assembly is presented. To simulate the PMSM drive system step by step algorithm is proposed and presented in form of flow chart in this dissertation work and discussed.

CONTENTS

LIST OF SYMBOLS

V_m	-	peak voltage
V_{as}, V_{bs}, V_{cs}	-	stator phase voltages of respective phases
i_{as},i_{bs},i_{cs}	-	stator phase currents of respective phases.
V_{ds},V_{qs}	-	d and q axis stator voltages
i_{ds}, i_{qs}	-	d and q axis stator currents.
V_c	-	Inverter dc input voltage
w_s	-	angular synchronous speed
w_r	-	angular rotor speed
r_1	-	stator resistance.
L_d,L_q	-	d and q axis inductances
L_{md}	-	d axis magnetizing inductance.
i_{fd}	-	d axis magnetizing current.
λds, λqs	-	d and q axis stator flux linkage
λaf	-	Flux linkage due to the rotor magnets linking the -
- stator		
Bg	-	air gap flux density.
lm	-	magnet thickness

lg	-	gap between the iron.
Te,Tl	-	electromagnetic and load torque
B	-	Viscous coefficient of the motor
Jm	-	moment of the inertia of motor
P	-	number of poles of motor.
p	-	differential operator (d/dt)
wr*	-	reference speed
Te*	-	torque command
i_s^*	-	stator current command.
$i_{as}^*, i_{bs}^*, i_{cs}^*$	-	three phase current commands.
$\Delta i_{as}, \Delta i_{bs}, \Delta i_{cs}$	-	three phase current deviations
Kp, K_i	-	proportional and integral constant of PI controller
h	-	hysteresis band
τ	-	free wheeling period.
T	-	sampling period
σ	-	relative stability
ζ	-	damping ratio

CHAPTER –1

INTRODUCTION

1.1 INTRODUCTION

The growing interest in energy saving especially in industrial applications, has led to explore in more details the potential of unconventional excitation systems for electric machines. The wide spread use of permanent magnet (PM) in dc as well as in synchronous machines, to substitute the excitation circuit, is one of the way followed to reach this objective. Over the past few years, PM motors have received much wide spread interest in many industrial applications. The PM motor has the potential to replace the induction and wound field commutator motor in a number of industrial, commercial and domestic variable speed drive area based largely on its energy saving capability. The PM motor has numerous advantages over other machines that are conventionally used for ac servo drives. The two most common on types of PM motors are classified as :

(1) Permanent Magnet Synchronous Motor (PMSM).

(2) Trapezoidal or Brushless DC motor (BDCM).

The PMSM has a uniformally rotating field as in an induction motor while the stator field of BDCM is switched in discrete steps. The PMSM and the BDCM have many similarities and differences.

1.1.1 Description of the Permanent Magnet Synchronous Motor and Brushless DC Motor

The PMSM owes its origin to the replacement of the exciter of the wound rotor synchronous machine, which included a field coil, brushes, and slip rings with a permanent magnet. A distinguishing feature of the PMSM is that it generates a sinusoidal back emf just like an induction motor or wound rotor synchronous motor, in fact, the stator of the PMSM is quite similar to that of the induction machine.

The BDCM owes its origin to an attempt to invert the conventional dc machine to remove the need for the commutator and brush gear. The commutator in the conventional dc machine converts the input dc current into approximately rectangular shaped currents of variable frequency. By applying this rectangular shaped current directly to the stator of the BDCM and transferring the field excitation to the rotor in the form of a permanent magnet, an inversion of the conventional dc machine has taken place with

the advantage that the new inverted machine does not have a mechanical commutator and brush gear, hence the name is brushless dc machine.

The PMSM has a sinusoidal back emf, whereas the BDCM has a trapezoidal back emf, Both have a permanent magnet rotor, but the difference is in the winding arrangement of the stator and shapping of the magnets. Sinusoidal stator currents are needed to produce a steady torque in the PMSM, whereas rectangular shaped currents are needed to produce a steady torque in the BDCM.

The magnets in the PMSM or the BDCM can be either buried or surface mounted. In the surface-mounted machine, two variations can exist. The Magnets can be inset into the rotor or project form the surface of the rotor. These machines will be referred to as buried, inset, and projecting PM machines respectively. Buried PM machines are more difficult to construct than either the inset or projecting surface mounted machines. In addition, an epoxy glue is used to fix the magnets to the rotor surface in the inset and projecting surface mounted machines. This implies that the mechanical strength of the surface mounted machines is only as good as that of the epoxy glue, assuming no retaining sleeve is used, hence, buried PM machines are more robust and tend to be used for high-speed applications.

1.1.2 : Advantages of PM machine over conventional machines

The PM machine has numerous advantages over other conventionally used machines.

(1) The rare earth and neodyminun boron PM machine has a lower inertia because of the absence of rotor cage, this makes for a faster response for a given electric torque. In other words, the torque to inertia ratio of these PM machines is higher.

(2) The PM machine has a higher efficiency, because there are negligible rotor losses in permanent magnet machines.

(3) All the conventional machines requires a source of magnetizing current for excitation, but the PM Machine already has the excitation in the form of rotor magnet.

(4) The PM machine is smaller in size than other machines of the same capacity. Hence, it is advantageous to use PM machines, especially where space is a serious limitation. In addition the PM machine has less weight. In other words, the power density of PM machine is higher.

(5) The rotor losses in an PM machine are negligible. A problem that has been encountered in the machine tools industry is the transferal

of these rotor losses in the form of heat to the machine tools and work pieces, thus affecting the machine operation. This problem is avoided in PM machines.

1.1.3 Advantages of conventional machines over PM machine

The conventional machine have following advantages over PM machine:

(1) Larger field weakening range and ease of control in that region

(2) Lower cogging torques

(3) less expensive feedback transducers such as an incremental rotor position encoder for the Induction motor instead of an absolute position encoder that is required by the PM motor drives.

(4) Lower cost

(5) Much higher rotor operating temperatures that are allowed in conventional machines than in PM machine

1.1.4 PM motor drive application

The specific positive characteristics of PM machines summarized earlier make them highly attractive candidates for several classes of drive applications, a few of which are discussed in this section

(1) Servo Actuators

The superior power density of PM machines is invaluable for applications which requires maximum dynamic response including machine tool servos and robotic actuator drives. The absence of rotor losses is another feature that makes PM motors attractive candidates for servos.

(2) Commercial -Residential Speed Control Applications

Opportunities for PM motor drives are also growing in a wide range of commercial and residential applications. For example, use of such drives is expanding in domestic appliances, ventilating and air-conditioning equipments. Trapezoidal PM motor drives have generally been the most popular choice for this class of cost-sensitive application to take the advantage of the simpler control and minimum sensor requirements associated with this type of machine, although PM motor drives have been under development for such applications for several years, cost reduction is the single largest challenge for achieving wider market acceptance of these drives in such high volume commercial - residential applications.

(3) Automotive Applications

Another application area for efficient variable speed drives with high market volume potential is electric vehicles. Sinusoidal PM machines are the clear favorite over their trapezoidal counterparts for the traction application because of the need for wide ranges of constant horsepower operation. Although the low-loss characteristics of PM machines make them appealing candidates for traction motors in battery supplied vehicles, this advantage can be compromised by the need to maintain high efficiency level over the complete speed range.

1.2 LITERATURE SURVEY

Interest in replacement of constant speed drives with variable-speed drives has increased considerable with the current concern for energy conservation and improved process efficiency. Traditionally, commutator machines were used for variable speed applications, but more recently, induction motors supplied by variable frequency inverters have become the more usual choice. Permanent magnet motors have been applied extensively in low power ratings for special performance drives but have not yet achieved wide application in the general drive market. They may however be preferred in the future for such applications due to their higher

efficiency, ease of position and speed control, dynamic torque capability and ruggedness.

Ashok B. Kulkarni and Mehrdad Ehsani [11] discuss a novel position sensor elimination technique for the interior PM synchronous motor drive. This paper investigates an indirect approach to position sensing. The IPM synchronous motor is characterized by the fact that its phase inductance varies appreciably as a function of the rotor position. This feature is utilized to get an estimate of the rotor position. The analytical equations are developed for the calculation of the phase inductance of an IPM motor drives by a current controlled PWM convertor with a hysteresis controller. The calculated phase inductance is then used to estimate the position of the rotor using a set a stored data relating the phase inductance and the rotor position.

M.F. Rahaman L.Zhong and K.W.Lim [12] described a direct torque-controlled interior permanent magnet synchronous motor drive incorporating field weakening. This paper presents a new control scheme for wide speed range operation of IPM synchronous motor drives. Where both torque and stator flux linkage are directly controlled. Current controllers followed by PWM or hysteresis comparators and coordinate transformation are not used. This eliminates the delays through these

networks and offers the possibility of dispensing with the rotor position sensor for the electronic commutator, if the initial rotor position is known as only approximately. The scheme incorporates all the usual control regimes, such as the maximum torque per ampere operation in constant torque region, the flux weakening region and operates the drive within the voltage and current limits of the motor/inverter.

Marco Bilewski and others [13] developed control strategies of an interior permanent magnet motor suitable for field weakening are considered. In this scheme a flux oriented frame is chosen based on flux observer. An allowable operating area in the state plane is selected and the related boundaries are implemented in the control scheme.

R. Krishnan and Shiyoung Lee[14] applied a new power converter topology to the PM Brushless DC motor drive. Cost minimization of the PMBDC motor drive is of immense interest to the industry at present, due to the opening up of a large number of applications to variable speed of operation.

M.J. corley and R.D. Lorenz [15] introduced the self-sensing ("sensor less") control of salient-pole PM synchronous motors. The major contribution of this work is the introduction of a simple-to-implement estimation technique that operates over a wide speed range, including

zero speed. The technique utilized the dependence of inductance on rotor position in interior PM machines to produce position and velocity estimates both for field orientation and for all motion control of the drives. The technique functions in a manner similar to a resolver and resolver to digital converter (RTDC) sensing system, whereby in the proposed technique the motor acts as the electromagnetic resolver and the power converter applies carrier-frequency voltage to the stator which produces high frequency currents that very with position. The sensed currents are then processed with a hetrodyning technique that produces a signal that is approximately proportional to the difference between the actual rotor position and an estimated rotor position.

Raymond B.Sepe and Jeffrey, H. Lang [16] presented a real-time adaptive control of the permanent magnet synchronous motor. They developed a fully digital adaptive velocity controller for the permanent magnet synchronous motor. The critical issues addressed during the development of this controller including discretization and global linearization of the nonlinear motor systems, nonlinearities in the inverter, nonminimum phase behavior due to sampling.

Raymond B. Sepe and Jeffrey. H. Lang [17] describe a real-time observer based (adaptive) control of a permanent magnet synchronous

motor without mechanical sensor. The control system utilizes a mechanically sensorless full-state observer for the generation of all controller feed back information.

Pragasen Pillay and Ramu Krishna [18] developed the application characteristics of permanent magnet synchronous and brushless dc motors for servo drives. For application considerations, these two motor drives have to be differentiated on the basis of known engineering criteria. Some of the criteria used to assess these two machines include power density, torque per unit current, speed range, feedback devices, inverter rating cogging torque and parameter sensitivity.

C.C. Chan and others [19] successfully applied a novel permanent magnet motor drives for electric vehicles to fulfil the special requirements such as high power density, high efficiency, high starting torque and high cruising speed. These PM motors are all brushless and consists of various types, namely rectangular fed, sinusoidal fed, surface magnet, buried-magnet, and hybrid.

1.3 AUTHOR'S CONTRIBUTION

The author has developed the software for the speed control of permanent magnet synchronous motor drives that is fed by a current hysteresis controlled voltage source inverter . The main objective to employ a current hysteresis controlled PWM VSI is the minimization of deviation between the reference three phase line current commands and the feedback three phase line currents through the switching of inverter power devices. The reference current commands are generated based on the principle that the resultant stator current vector is always kept in quadrature with the rotor flux vector.

A detailed literature survey is reported in the proposed work area in chapter I. The characteristics of permanent magnet materials provides a basis for appreciating the potential and limitations of PM machines. The chapter II describnes the characteristics of some important permanent magnet materials. A simple construction equivalent circuit and operating characteristics are also included in this chapter. A general description of proposed speed control system and mathematical modeling of PMSM and controllers are given in chapterIII. Chapter IV provides both determination of controller parameter and computer simulation of speed control system. The parameter of the PI speed controller are designed on the basis of

system stability and response of the drive system. The simulated results are presented in chapter V. The chapterVI gives the overall conclusion of the developed drive system and scope for further work.

CHAPTER – 2

PERMANENT MAGNET AC MOTORS

PMAC machine represent the convergence of at least two distinct-theory of permanent magnet machine development. One of these threads is the development of line-start PMAC motors with embedded rotor squirrel cage windings designed for operation directly from utility-supplied AC power. This class of hybrid PMAC induction machines were using Alnico magnets. These machines were widely applied in some important industrial applications such as textile manufacturing lines that require large number of machines operating at identical speeds. Later during the 1970s, considerable research attention was focused on improved designs for line-start PMAC machines as a means of achieve significant energy savings in industrial applications. Integral horsepower variety of these line-start PMAC motors have been developed with impressive efficient characteristics using ferrite and rare earth magnets, but their manufacturing cost oyer conventional induction machines prevent wide market acceptance. Nevertheless, significant technical progress has been demonstrated in the development of these high-power PMAC machines, and continues today.

Representing the second thread of development, permanent magnet dc (PMDC) servo motors began to replace conventional wound-field dc motors in high- performance machine tool servo applications in the 1960s when solid-state dc chopper circuits reached market maturity. The availability of high-strength rare earth permanent magnets made it possible to develop compact fast response PMDC servo motors without the steady state losses and additional circuit complications associated with traditional wound-field dc machine.

Finally, in the 1970s, these two development paths converged as PMAC machines (without rotor cages) were combined with adjustable frequency inverter to achieve high performance motion control. This approach had the desirable effect of eliminating the dual disadvantages of high rotor inertia and brush wear associated with PMDC motor commutators. The class of brushless dc motors using trapezoidal PMAC motors was developed first in order to take advantage of the control simplifications that are achievable with this configuration. This has been followed by the evolution of high performance sinusoidal PMAC machine during the late 1970s, and 1980s which have been made possible by the rapid advances in digital real- time control, hardware and vector control technology first applied to induction motors.

The permanent magnets are the vital components of PM machines. The characteristics of permanent magnet materials provide a basis for appreciating the potential and limitations of PM machines. Developments in metallic permanent magnets have taken place in quantum steps with the introduction of new families of magnets. The production of semi-hard and hard permanent magnets has been increasing steadly. These magnets are widely used in various fields of electrotechnology. Of all these materials Alnico, ferries and Samarium-cobalt magnets have major impact. Fig. 2.1 shows the historical development of maximum energy product of commercial permanent magnets. It is evident that a nearly- exponential increase is occurring with the introduction of the new ternary compounds containing Nd, B, and Fe. These exhibit remarkable magnetic and physical properties, promising extensive application in electro-mechnical energy conversion devices.

2.1 MAGNETIC MATERIALS

Three basic magnetic parameters are of critical importance for PM applications in machines. These are residual flux density B_r, coercive force H_c and maximum energy product (BH_{max}). It is the value of B_r which primarily determines what magnet area perpendicular to the main flux path

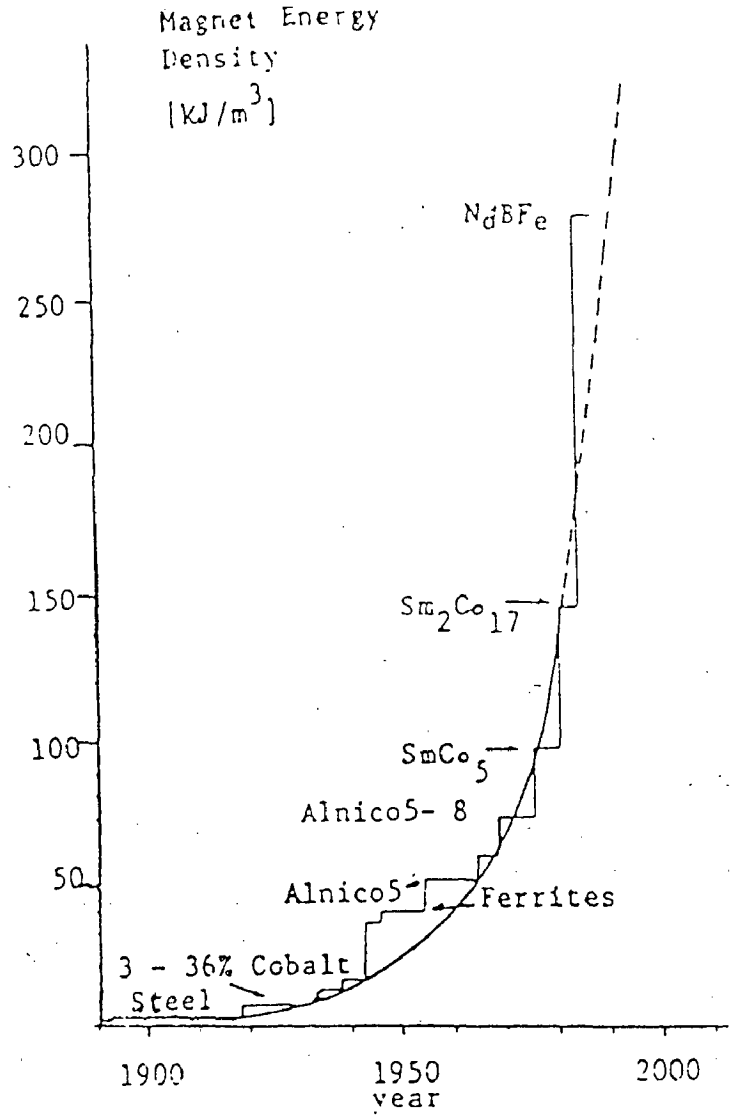

Fig. 2.1 : Increase in maximum energy product (BH_{max}) for commercial permanent magnet materials.

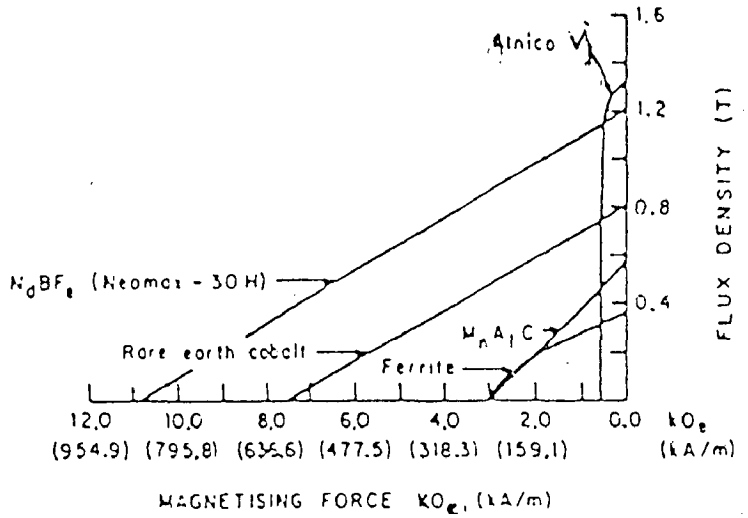

Fig. 2.2 : Second Quadrant B-H Characteristics of Magnet Materials

is required to mainttain the air gap operating flux. The coercive force H_c gives a first-order measure of the magnet's resistance against demagnetization during short-circuit, starting, etc. The (BH_{max}) product is inversely related to the total magnet volume required for a given application. Tablel contains pertinent properties of several permanent magnet materials.

Table - I

Properties of Permanent Magnets

Material	Br (T)	Hc (KA/m)	(BH_{max}) W(KJ/m^3)	Remarks
Alnico V	1.280	51	44	Brittle and hard to machine
Ferrites	0.385	235	28	Brittle and hard to machine
Mn-Al-C	0.560	239	61	Ductile, Machinable
$SmCO_5$	0.87	637	146	Brittle,difficult to machine
$Nd_{15}B_8Fe_{77}$	1.23	881	290	Machinable, 150°C limit

A most important property for successful application of permanent magnets in electrical machines is the linearity of the demagnetization curve in the second quadrant. Fig. 2.2 shows the 2nd quadrant of the B-H curves for several permanent magnet materials. For the ferrites, samarium cobalt

and neodymium boron iron, it is noted that the demagnetization curve is essentially linear over the whole of the second quadrant. When such materials are subjected to a demagnetizing field within this linear range, the recoil characteristic is near identical with the demagnetization curve and there is no loss of residual magnetism. It is only if demagnetization is carried into the curved portion that permanent loss of magnetization occurs. The relative recoil permeability of these material in the linear region is little greater than unity. For the neodymium iron material, it is about 1.05. In contrast, the Alnico V material has no substantial linear position and loses permanent magnetism for any reverse field. Its recoil line is however reasonably linear with a relative permeability in the range 3.5-5. The design must be such that the demagnetization is limited to the linear part of the B-H characteristics.

Cost and security of supply of raw materials are two major constraints on the application of newer magnetic materials in commercial machines. For samarium cobalt, the cost is relatively high and the future security of supply of both samarium and cobalt is questionable. The iron-based neodymium boron materials offer both a lower cost (comparable with Alnico's per unit weight) and plentiful material supply. Large scale application, as in the automotive industry, is therefore conceivable. Now a days, the major limitation on the application of neodymium iron magnets is

the limited temperature tolerance. While the Curie temperature is about 300°C, operation must normally be limited to about 150°C because of the relatively high temperature coefficient of residual flux density above that temperature.

2.2 PERMANENT MAGNET SYNCHRONOUS MOTOR

Permanent magnet synchronous motors (PMSMs) are finding many applications in various fields especially for high performance electric drives. Compared with other electric machines, PMSMs combine the advantages of both conventional sycnhronous machines and induction machines, featuring high efficiency and power factor, low maintenance requirements, small size and low weight for a given rating. PMSMs are made in a number of configurations. One of the simplest with surface magnet is shown in cross section in Fig. 2.3.

The rotor has an iron core that may be solid or may be made of punched limitations for simplicity in manufacture thin permanent magnets are mounted on the surface of this core using adhesives. Alternating magnets of the opposite magnetization direction produces radially directed flux density across the air gap. This flux density then reacts with currents in

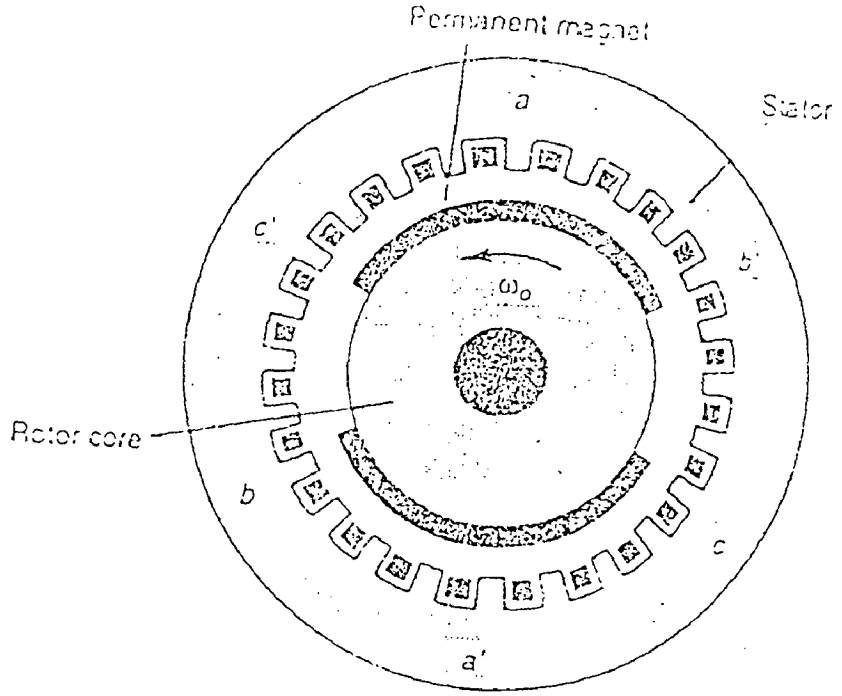

Fig. 2.3 : Cross section of permanent magnet motor.

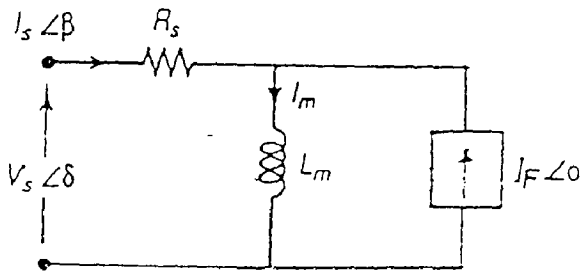

Fig. 2.4 : Equivalent circuit for PM motor.

windings placed in slots on the inner surface of the stator to produce torque.

2.2.1 Equivalent Circuit

The stator of synchronous type PM motor shown in Fig. 2.3 is essentially identical to that of an induction motor. The three windings are each distributed to provide a near-sinusoidal distribution of linear current density around the air-gap periphery so that a set of phase current sinusoidally varying in time, will set up a field that is sinusoidally distributed peripherally and is rotating at an angular velocity of $(2/p)w_s$. The air-gap flux density Bg can therefore be approximated by

$$Bg = Br\frac{lm}{lg} \quad T$$

The flux density production by the magnets is a rectangularly distributed wave of relatively constant magnitude over the magnet surface, alternating in polarity with adjacent magnet poles. To the extent that the stator windings are approximately sinusoidally distributed, only the fundamental space component of the magnet flux density wave can link with the stator windings. The magnitude of this component is proportional

to sin α, where α is the half angular width of the magnet measured in electrical radius. A typical value of α for PMSM is about $\pi/3$ rad, that is a magnet coverage of two-thirds of the rotor surface. At this value, the rms gap flux density is 0.78 of the peak gap density. When the rotor rotates at angular velocity w_r, the effect of the rotor as seen by the stator can be represented as a sinusoidal current source with an angular frequency $w_s = (P/2)\, w_r$ for a P-pole motor.

The steady- state equivalent circuit is shown in Fig. 2.4. The stator current phasor is $I_s \angle\beta$, where the phase angle β is the electric angle by which the peak field of the stator leads the rotor magnet axis, which in turn is related directly to the angular position of the rotor. The magnetising inductance Lm for the PM motor is much smaller than that of an induction motor with the same stator because the effective magnetic gap lg between the stator iron and the rotor iron is much larger, the magnet material having a permeability approximately equal to that of air. Thus the magnetizing current Im is usually in the range 2-5 times rated stator current in contrast with the range 0.2-0.5 for induction motors. Typically the current I_F has a magnitude of 2-5 times rated current.

2.2.2 Operating Characteristics

A PM synchronous motor provides continuous torque only when the speed is directly related to the supply frequency. The supply may be either a three phase controlled voltage or controlled current. Many synchronous PM drives are used with a rotor position sensor from which the rotor angle can be obtained. The stator voltages or current are then constructed by switching action of the inverter to have the desired wave shape and the desired relative instantaneous phase angle. For the current source drive using the equivalent circuit of Fig.2.4 the torque can be derived as

$$T = \frac{3P}{2} \; Lm \; I_F \; I_s \; \sin\beta \quad N-m$$

Fig. 2.5 shows the torque as a function of the angle β with constant magnitude of stator current. For a given value of stator current maximum driving torque can be obtained with a rotor angle of $\beta = 90^\circ$. For this condition the electrical variables are displayed in the phasor diagram of Fig. 2.6 (a). This mode of operation gives maximum torque per ampere of stator current and therefore a high efficiency. However the supply power factor is seen to be less than unity. Operation in this condition is practical and preferred up to the speed at which the voltage limit of the inverter is reached. Above this, speed, a more appropriate operating conditions is

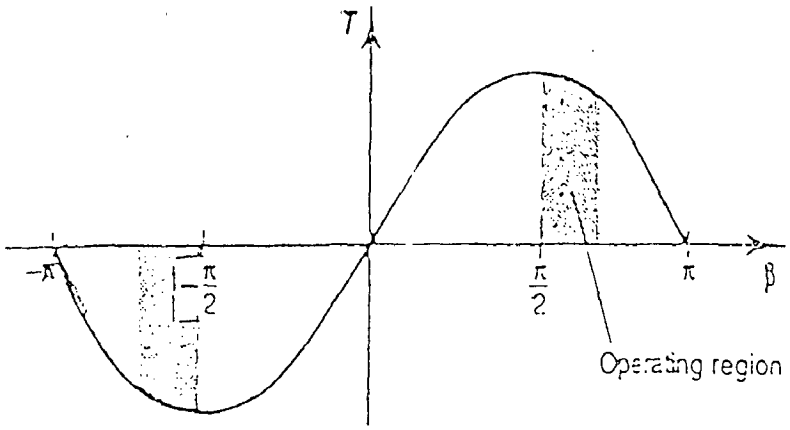

Fig. 2.5 : Torque-angle relation for PM motor.

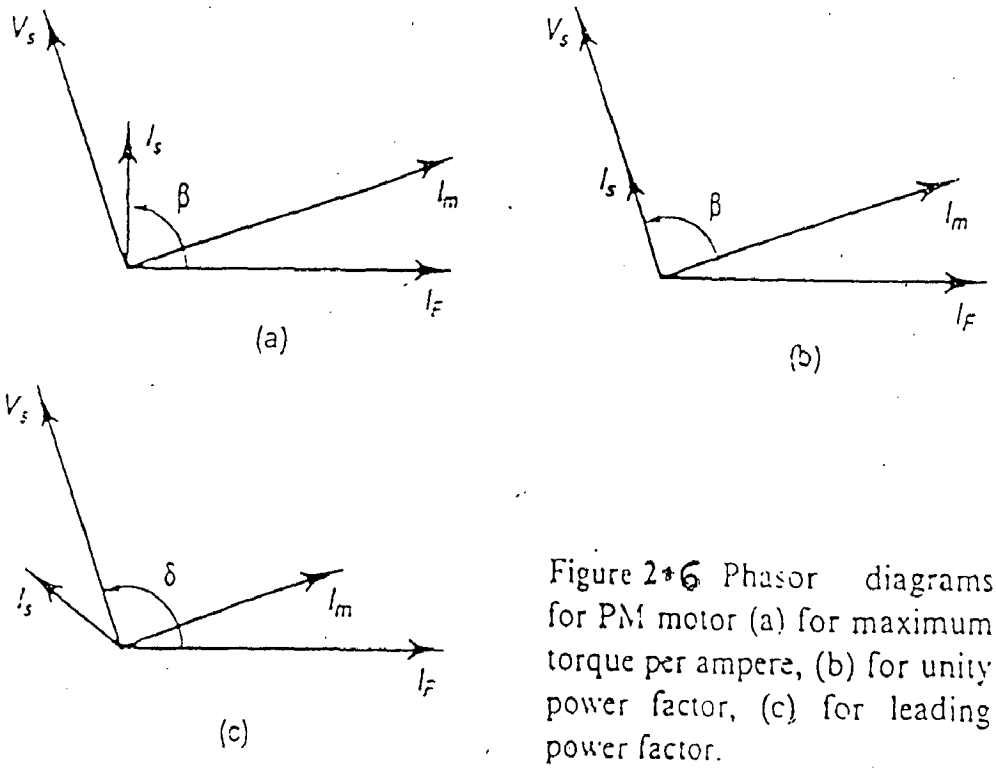

Figure 2.6 Phasor diagrams for PM motor (a) for maximum torque per ampere, (b) for unity power factor, (c) for leading power factor.

one which provides for unity power factor this maximizing the utilization of the inverter voltanpere rating. This is achieved by increasing the current lead angle β as shown in phasor digram of Fig 2.6 (b). For regeneration, the rotor angle β is made similarly negative.

For a voltage-driven PM drive, the magnitude of the supply voltage and its frequency are made proportional to the motor speed. Operating conditions equivalent to those of Fig. 2.6(a) & (b) can be employed by appropriate adjustment of the angle δ by which stator voltage phasor leads the field axis. However, the motor can also be operated with a leading or capacitive stator current by increasing the load angle δ as shown in Fig. 2.6 (c). This condition is particularly desirable for some large drive since it allows use of a load commutated inverter, that is, one where the switches are turned off by their current going to zero rather than requiring auxiliary turn off means.

2.2.3 Magnet Protction

Demagnetization of a part of the magnet can occur if the flux density in that part is reduced to less than the knee point flux density. This can result in permanent reduction in torque capability since it is usually not feasible to remagnetize the magnets without disassembly of the motor. As

seen in the phasor diagram of Fig. 2.6, the stator current in the driving mode is normally controlled to lead the effective magnet current by 90° or more. The effect of this stator magnetic field is to increase the air-gap flux density near the leading edge of each magnet and decreases it near the lagging edge. With normal values of stator current, the effect of the air-gap flux in producing torque is relatively unchanged. The limiting value of permissible stator current is that which brings the flux density down to the value B_d at the lagging edge. Most PM motors are designed to with stand considerable overload currents without danger to the magnets. The safe value of the stator current is usually can exceed the magnetizing current Im without causing demagnetization, it is be typically 2-5 times the rated stator current.

The major danger to the magnet may arise from a short-circuit on the stator terminals as a result of a failure in the inverter. The stator and magnet fields will oppose each other directly, causing the greatest reduction in flux density at the magnet center. If the limiting magnet flux density B_d is zero or negative, this steady state short-circuit current can usually be tolerated without damage. However, the steady- state component of the short-circuit current space vector is accompanied by an initial transient space vector component of equal instantaneous magnitude. This transient decays at a time constant Lm/r_1, where r_1 is the stator resistance. In small

machines, this constant is so small in relation, to a half period of the maximum fundamental frequency that it has little effect. However, in large motor, the time constant may be several periods in length and the demagnetizing effect of the short-circuit current may be nearly doubled. For these motors, one means of providing the required protection is to design for additional stator leakage inductance or to add external series inductance.

2.2.4. Losses and Efficiency

Synchronous PM motors are potentially much efficient than induction motors. There is no equivalent of the loss in the rotor bars of the induction motor. Also, the stray losses that result mainly from magnetic interaction of the closely adjacent stator and rotor in the induction motor are effectively eliminated by the large iron-to-iron gap of the PM motor. With modern magnet materials, the resistivity is such that losses due to tooth ripple variations in the air-gap flux density produce little loss in the magnet material for most designs. This loss may, however, becomes significant for motors operated at very high frequencies and speeds. This leaves the stator core loss, the stator winding loss and the windage and friction loss.

Let us compare PM and induction of the same frame size and shape. At the same speed, the friction loss in the bearings will be similar for the two motors. The windage of the PM motor may be some what reduced due to the reduced need for an internal fan in totally enclose motor than has negligible rotor heating. For the same maximum flux density, the hysteresis component of the core loss in a synchronous PM motor will be the same as that of an induction motor, but the eddy current component will be higher. This is mainly due to the rapid rise and fall in the flux density of the stator teeth as each magnet edge passes into or out of the space under a tooth. The eddy current iron loss can be minimized by appropriate choice of the iron lamination material and also by designing with a smaller number of wider teeth per pole. In addition, the rate of change of tooth flux density can be reduced by beveling the magnet edges. Typically, the PM motor core loss may be in the range 1.25-2.0 times that of a machine with near sinusoidal flux distribution.

The PM motor can be operated at unity power factor, while the induction motor will always have a lagging power factor, typically in the range 0.8-0.9 for four-pole motors and lower for large number of poles. For the same input power rating, the ratio of the stator currents of the PM and induction motors will be small with this power factor. Thus, the ratio of the stator winding losses for the PM and induction motors will be the induction

motor power factor squared. For the same power rating, the total losses in the PM motor will typically be about 50-60% of those of the induction motor. Predicted values of PM motor efficiency are about 95-97% for rating in the range10-100 KW as compared with 90-94% for induction motors. Also the reduction in PM motor efficiency with reduction in speed will be less than experienced with induction motors. The overall drive efficiency is further improved because the rating, and therefore the loss in the inverter will be reduced roughly in proportion to the power factor.

With PM motors, the number of poles can be chosen to optimize the efficiency. Increasing poles increases the frequency and thus the core loss per kilogram of stator iron. However, the thickness and mass of the stator yoke is reduced in approximately inverse proportion to the pole number, partially compensating for the effect of increased frequency. Also, the decrease in yoke thickness allows an increase in the rotor radius for a given overall frame size. This allows the required torque to be produced by a shorter motor. An additional advantage of increased pole number is the shortening of the end turns of the stator winding reducing the stator resistance and therefore the loss. From an efficiency stand point, the optimum number of poles is frequently in the range 8-12.

2.3 BRUSHLESS DC MOTOR

The other major class of PM motor drives is alternatively known as trapezoidally excited PM motor or brushless d.c. motor, or simply as switched PM motors. Normally, these have stator windings that are supplied in sequence with hear rectangular pulses of current. A cross section of one type of motor is shown in Fig. 2.7. In most respects, this switched motor is identical in form with the synchronous PM motor. The characteristic features of the brushless dc motors are :

(i) rectangular distribution of magnet flux in the air gap.

(ii) rectangular current wave forms.

(iii) Concentrated stator windings.

The stator winding of brushless dc motor may be star or delta connected.

Star-Connected

These windings are generally similar to those of an induction or synchronous motor except that the conductors of each phase winding are full pitched, that is, they are distributed uniformally in slots over two stator

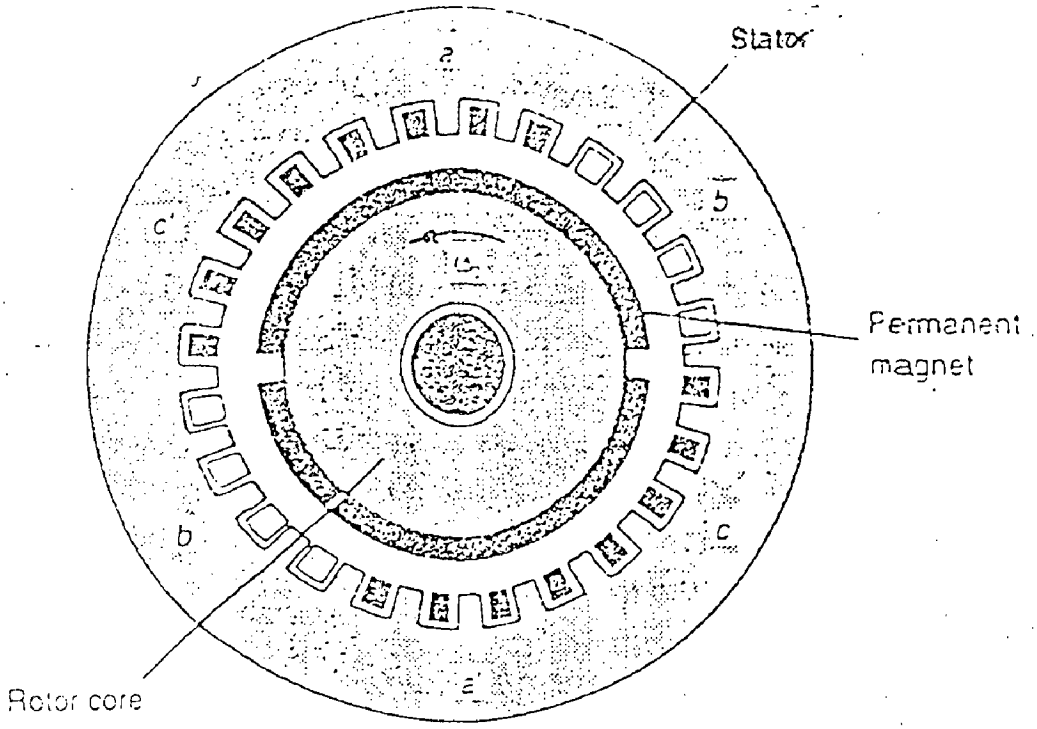

Fig. 2.7 : Cross section of a switched PM motor.

arcs each of 60°. The electrical supply system is designed to provide a current that can be switched sequentiallly to pairs of the three stator terminals. The sequence of switching actions can be simply trigged by the use of signals from position sensors (e.g. Hall sensors) mounted at appropriate positions around the stator. Six steps of this switching cycle are required per revolution for a two pole motor.

Delta Connected

An alternate form of brushless dc motor has magnets that are typically about 120° in angular width rather than 180°. In this type, current is supplied in a switched sequence into one stator terminal and out another. At any instant , approximately two-thirds of this current flows through one phase winding while one-third flows through the other two phases in series.

The development and characteristics of some important permanent magnetic materials are described in this chapter. The remarkable magnetic and physical properties of Nd-B-Fe promising extensive applications in electro-mechanical energy conversion devices. The simple construction, equivalent circuit and operating characteristics of both permanent magnet synchronous motor and brushless dc motor are also included in this chapter.

CHAPTER - 3

MATHEMATICAL MODELING OF PERMANENT MAGNET SYNCHRONOUS MOTOR DRIVE

The PMSM has numerous advantages over other machines that are conventionally used. The stator current of an induction motor (IM) contains magnetizing as well as torque producing components The use of the permanent magnet in the rotor of the PMSM makes it unnecessary to supply magnetising current through the stator for constant air-gap flux. The stator current need to be only torque producing. Hence for the same output, the PMSM will operate at higher power factor (because of absence of magnetizing current) and will be more efficient than IM. The conventional wound rotor syncbronous machine (SM), must have dc excitation on the motor, which is often supplied by brushes and slip rings. This implies rotor losses and regular brush maintenance. The key reason for the development of the PMSM was to remove the foregoing disadvantages of the SM by replacing its field coil, dc power supply, and slip rings with a permanent magnet. The PMSM, therefore, has a sinusoidal induced emf and requires sinusoidal currents to produce constant torque just like the synchronous machine.

3.1 SYSTEM DESCRIPTION

The block diagram for the proposed system is shown in Fig. (3.1). The system consists of a three-phase PMSM and load, a current hysteresis-controlled PWM VSI with three-independent phase controls, and a three - phase sinusoidal current reference generator that received amplitude and phase commands of the stator current vector from the digital controller. The motor chosen for the study is a three-phase y-connected four pole Electro-Craft BLM-2004 PMSM with a trapezoidal air gap magnetic flux distribution. A resolver is mounted on the motor shaft for velocity and position sensing. The output of the resolver is converted into digital rotor speed and absolute rotor position values using a resolver to digital converter (RDC). The motor does not utilize a conventional commutation sensor or a brushes tachometer for determining the absolute rotor position. The digital controller uses feed back RDC information the sensed three-phase line current, and the input reference speed to generate amplitude and phase commands for the sinusoidal current reference generate.

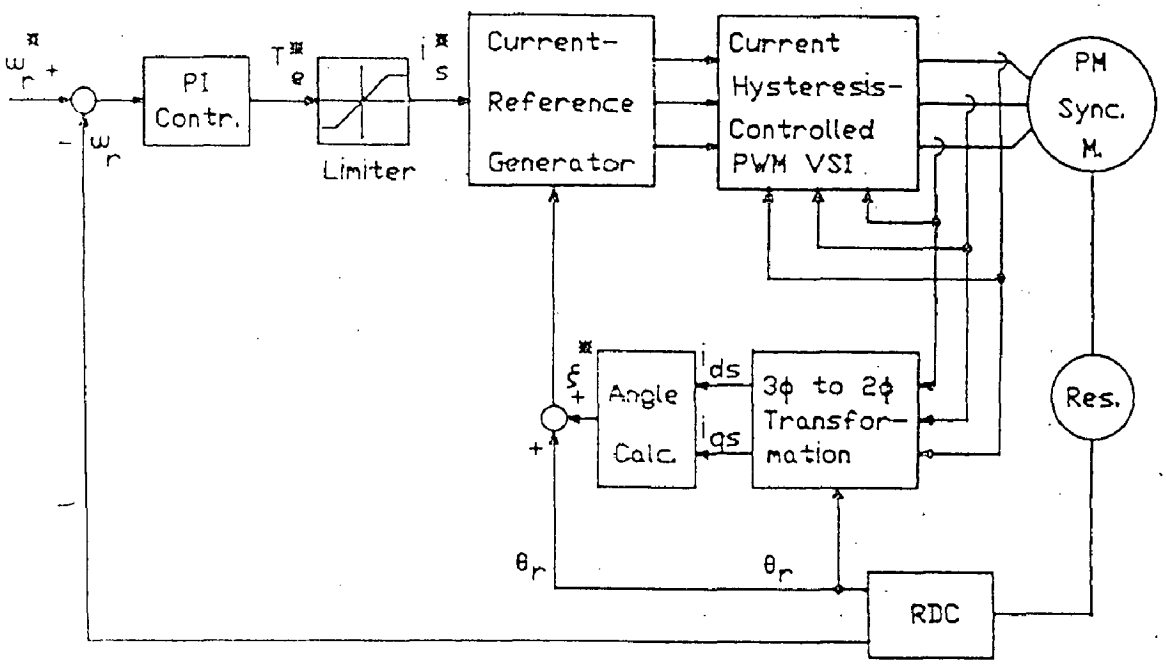

Fig. 3.1 Block diagram for the proposed digital speed control system.

3.2 MATHEMATICAL MODELING OF PMSM DRIVE

The system consists of three phase PMSM and load, a current hysteresis controlled PWM VSI with three independent phase controls, and a three phase sinusoidal current reference generator that received amplitude and phase commands of the stator current vectro from the digital controller.

3.2.1. Machine Model

The stator of the PMSM and the wound rotor SM are similar. The permanent magnets used in the PMSM are of a modern rare-earth variety with high resistivity, so induced currents in the rotor are negligible. In addition, there is no difference between the back emf produced by a permanent magnet and that produced by an excited coil. Hence the mathematical model of the PMSM is similar to that of the wound rotor synchronous machine. The following assumptions are made in the derivation.

1. Saturation is neglected although it can be taken into account by parameter changes.
2. The induced emf is sinusoidal.

To achieve the required control approach, the digital speed control in Fig. (3.1). The system is assumed to be operate under a uniform sampling rate. In each sampling period, the deviation between the reference speed w_r^* and the feedback motor speed w_r is processed by a digital PI control algorithm that generates the torque command Te*

Let $\Delta w_r = w_r^* - w_r$.

$$\frac{T_e^*(z)}{\Delta w_r(z)} = K_p + \frac{Ki}{(1-Z^{-1})}$$

taking the inverse z - transform of (3.14)

$$T_e^*(kT) = K_p \Delta w_r(kT) + Ki \sum_{i=0}^{k} \Delta w_r(iT) \quad \text{.....(4.1)}$$

for k = 1,2.....

where T is the sampling period.

Define a new variable

$$\alpha(kT) = \sum_{i=0}^{k} \Delta w_r(iT)$$

Where $\Delta w_r(0) = 0$

Equation (4.1) can be rewritten as

$$T_e^*(kT) = K_p \Delta w_r(kT) + Ki\alpha(kT) \quad \text{.....(4.2)}$$

and $\alpha(0) = 0$

This T_e^* (kT) is passed through a limiter to form the magnitude i_s^* of the stator current vector. i_s^* and T_e^* are related by

$$i_s^* = \begin{cases} T_e^*, \max & T_e^* \geq T_e^*, \max \\ T_e^* & -T_e^*, \max \leq T_e^* \leq T_e^*, \max \\ -T_e^*, \max & T_e^* \leq T_e^*, \max \end{cases} \qquad (4.3)$$

In order to accurately identify the position of the stator current vector in the d-q coordinate frame, the absolute rotor position and the angle must be determined. The absolute rotor position is measured by using the resolver mounted on the motor shaft and the RDC. The d-axis and the rotor flux positions are determined accordingly, since they all align with the absolute rotor position. The angle is computed via the three phase to two phase transformation of the stator line currents. Let i_{as}, i_{bs} and i_{cs} be the three phase stator line currents that are obtained by using current sensors. The two axis stator currents i_{ds} and i_{qs} are computed

$$\begin{bmatrix} i_{ds} \\ i_{qs} \\ 0 \end{bmatrix} = \frac{2}{3} \begin{bmatrix} \mathrm{Cos}\theta r & \mathrm{Cos}(\theta r - \frac{2\pi}{3}) & \mathrm{Cos}(\theta r + \frac{2\pi}{3}) \\ \mathrm{Sin}\theta r & \mathrm{Sin}(\theta r - \frac{2\pi}{3}) & \mathrm{Sin}(\theta r + \frac{2\pi}{3}) \\ \frac{1}{2} & \frac{1}{2} & \frac{1}{2} \end{bmatrix} \begin{bmatrix} i_{as} \\ i_{bs} \\ i_{cs} \end{bmatrix}$$

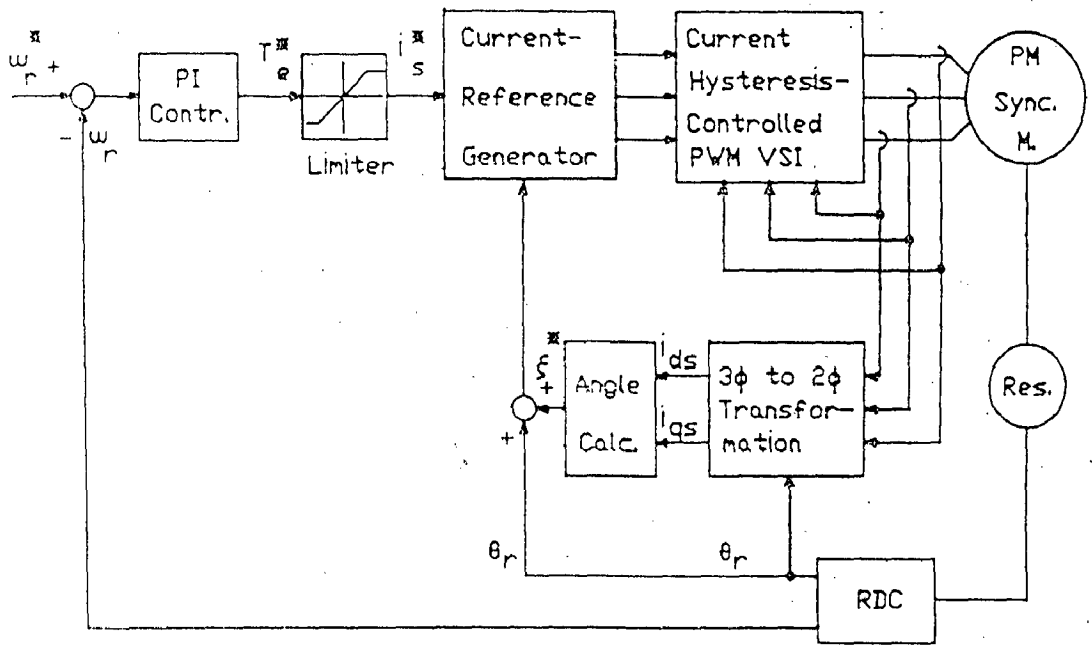

Fig. 3.1 Block diagram for the proposed digital speed control system.

3.2 MATHEMATICAL MODELING OF PMSM DRIVE

The system consists of three phase PMSM and load, a current hysteresis controlled PWM VSI with three independent phase controls, and a three phase sinusoidal current reference generator that received amplitude and phase commands of the stator current vectro from the digital controller.

3.2.1. Machine Model

The stator of the PMSM and the wound rotor SM are similar. The permanent magnets used in the PMSM are of a modern rare-earth variety with high resistivity, so induced currents in the rotor are negligible. In addition, there is no difference between the back emf produced by a permanent magnet and that produced by an excited coil. Hence the mathematical model of the PMSM is similar to that of the wound rotor synchronous machine. The following assumptions are made in the derivation.

1. Saturation is neglected although it can be taken into account by parameter changes.
2. The induced emf is sinusoidal.

3. Eddy currents and hysteresis losses are negligible.
4. There are no field current dynamics.
5. There is no cage on the rotor.

The stator voltage of the PMSM are :

$$V_{as} = V_m \text{ Cos } wt$$

$$V_{bs} = V_m \cos (wt - 2\pi/3) \qquad (3.1)$$

$$V_{cs} = V_m \cos (wt + 2\pi/3)$$

The d, q variable are obtained from a,b,c variables through the park transformation, given below :

$$\begin{bmatrix} Vqs \\ Vds \\ Vos \end{bmatrix} = \frac{2}{3} \begin{bmatrix} \cos\theta & \cos(\theta - \frac{2\pi}{3}) & \cos(\theta + \frac{2\pi}{3}) \\ \sin\theta & \sin(\theta - \frac{2\pi}{3}) & \sin(\theta + \frac{2\pi}{3}) \\ 1/2 & 1/2 & 1/2 \end{bmatrix} \begin{bmatrix} Vas \\ Vbs \\ Vcs \end{bmatrix} \qquad (3.2)$$

The stator d, q equations of the PMSM in the rotor reference frame are,

$$V_{qs} = r_1 i_{qs} + p\lambda_{qs} + w_s \lambda_{ds} \qquad (3.3)$$

$$V_{ds} = r_1 i_{ds} + p\lambda_{ds} - w_s \lambda_{qs} \qquad (3.4)$$

Where

$$\lambda_{qs} = L_q i_{qs} \qquad (3.5)$$

$$\lambda_{ds} = L_d i_{ds} + \lambda_{af} \qquad (3.6)$$

The electromagnetic torque is ,

$$Te = \left(\frac{3}{2}\right)\left(\frac{P}{2}\right)\left[\lambda_{ds} i_{qs} - \lambda_{qs} i_{ds}\right] \qquad (3.7)$$

$$Te = \left(\frac{3}{2}\right)\left(\frac{P}{2}\right)\left[\lambda_{af} i_{qs} + (L_d - L_q) i_{ds} i_{qs}\right] \qquad (3.8)$$

The equation of motor dynamics is

$$Te = T_L + Bw_r + J_m\, pw_r \qquad (3.9)$$

The inverter frequency is related to the rotor speed as follows :

$$w_s = \frac{P}{2} w_r \qquad (3.10)$$

From equation (3.3) - (3.9) we get

$$pw_r = (T_e - T_L - Bw_r)/J_m \ldots\ldots\ldots\ldots \qquad (3.11)$$

$$pi_{ds} = (V_{ds} - r_1\, i_{ds} + w_s\, L_q\, i_{qs})/L_d \ldots\ldots\ldots \qquad (3.12)$$

$$pi_{qs} = (V_{qs} - r_1 i_{qs} - w_s L_d\, i_{ds} - w_s \lambda_{af})/L_q \ldots\ldots\ldots \qquad (3.13)$$

Equations (3.11)-(3.13) represents three state (w_r, i_d, i_q) non-linear differential equations. The nonlinear model of the PMSM will be used in the numerical simultation of the drive performance.

3.2.2 Control Philosophy

The method of controlling the PMSM drive can be described by using the vector diagram shown in Fig. (3.2) and the field orientation principle. In Fig. (3.2) with the as-axis being the fixed reference axis, at steady -state, the d-q axes revolves around the air-gap in synchronism with synotronous speed. since in the PMSM the magnetic flux generated from the rotor is in fixed relation with rotor, the flux angular position is determined by the rotor position, which is in alignment with the d-axis. In the d-q coordinate frame the stator current i_s has two components ids and i_{qs}, where i_{ds} is the flux producing component. The angle between i_{ds} and i_{qs} is computed from $\xi = \tan^{-1}(i_{ds}/i_{qs})$. If by properly controlling the angle ξ so that the stator current vector is all transformed to the q-axis and i_{ds} is zero, the air-gap flux will be completely determine by the rotor magnet whose flux is the constants λds. According to (3.7) the generated torque Te is now linearly proportional to i_{qs}. Thus, direct torque control of the motor can be achieved, if the phase-angle of i_s with reference to the d-q coordinate frame is adjusted according to the condition $\xi = 0$ and the magnitude of i_s is adjusted according to the torque demand.

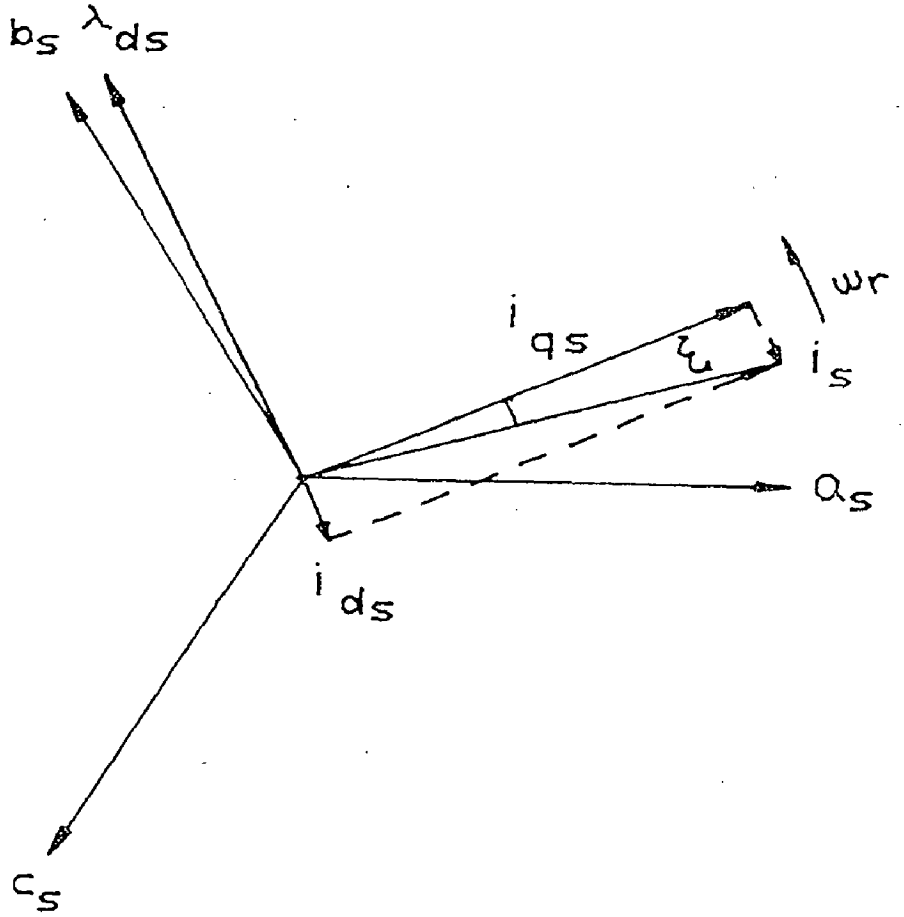

Fig. 3.2 The vector diagram for controlling the PMSM

3.2.3 Modeling of Speed Controller

To achieve the above control approach, the digital speed control system for PMSM drive is proposed as shown in Fig. (3.1). The systems is assumed to operate under a uniform sampling rate. In each sampling period, the deviation between the reference speed w_r^* and the feedback motor speed w_r is processed by a digital PI control algorithm that generates the torque command Te*.

Let $\Delta w_r = w_r^* - w_r$.

In the Z-domain

$$\frac{T_e^*(z)}{\Delta w_r(z)} = K_p + \frac{K_i}{(1-z^{-1})} \qquad (3.14)$$

Where Kp and K_i are the PI controller parameters.

3.2.4 Hysteresis Current Controllor

The principle employed in this system consists of controlling the inverter switches in such a way as to force the currents in the machine to follow references generated from a rotor position encoder. This type of control is easy to realize with a high frequency solid state devices where high switching frequencies are possible. In addition, it offers the interesting

possibility of direct torque control not only in steady state but also in transient operation (if the machine has no damping circuits).

From Fig. (3.1) the current reference generator generates the three-phase line current commands which serve as references for the hysteresis controlled PWM VSI. The basic circuit of a three-phase VSI is shown in Fig.(3.3). The three pairs of power switches (denoted by T_1-T_1', T_2=T_2' and T_3-T_3') provide eight conduction modes according to the switching of devices that is determined from the hysteresis controllers. Table II summarizes the eight conduction modes of the inverter. In table II, 1 denotes the ON state and O denotes OFF state of switches. For the conduction mode N_s = 6 and N_s=7, the three switches situated on the same side of the inverter are turned OFF or ON simultaneously. In either cases, the machine is disconnected from the inverter. These modes are called free wheeling periods and are indicated in table II by the index FW = 0, the rest of the modes are indicated by FW=1. The first six conduction modes in table II provide six non zero voltage vectors, while the last two modes provide zero voltage vectors. By properly applying the firing sequences (N_s=0 to N_s=5) to the inverter switches according to table II, the resultant stator voltage vectors and consequently stator current vectors will interact with the rotor flux to provide necessary electromagnetic torque for rotor motion.

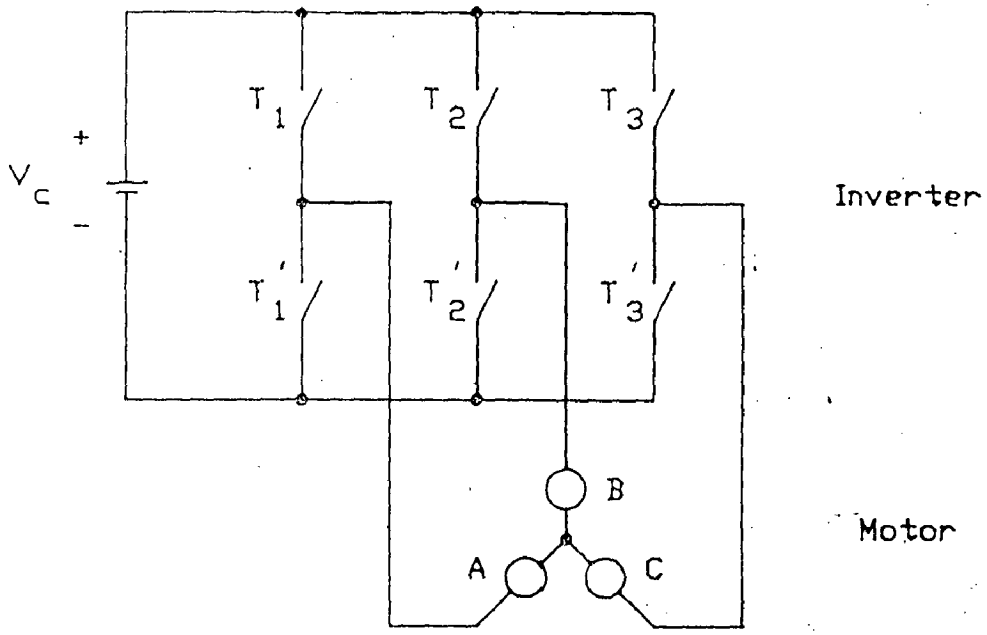

Fig. 3.3 The power circuit of a voltage-source inverter.

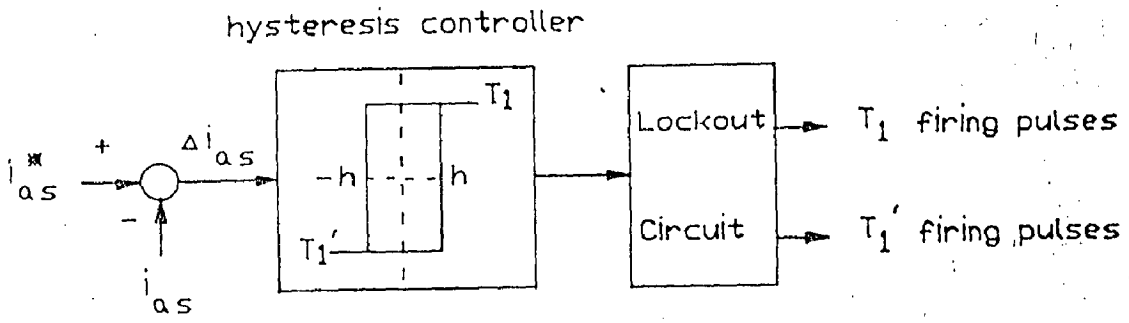

Fig. 3.4 Current hystresis controller for one inverter leg.

Table II

CONDUCTION MODES OF THE VSI

N_S	T_1	(T_1)	T_2	(T_2)	T_3	(T_3)	FW
0	0	(1)	0	(1)	1	(0)	1
1	1	(0)	0	(1)	1	(0)	1
2	1	(0)	0	(1)	0	(1)	1
3	1	(0)	1	(0)	0	(1)	1
4	0	(1)	1	(0)	0	(1)	1
5	0	(1)	1	(0)	1	(0)	1
6	0	(1)	0	(1)	0	(1)	0
7	1	(0)	1	(0)	1	(0)	0

The switching of the power switches is determined from the current hysteresis controllers. We are using three independent phase current controllers. Fig. (3.4) shows the control for one inverter lag. In this figure, the phase-a current reference i_{as}^* is subtracted from the feedback phase-a motor line current i_{as} to form the current deviation Δi_{as} ($=i_{as}^*- i_{as}$). If Δi_{as} is greater (less) than the preset hysteresis band to the inverter leg is switched in the positive (negative) direction, otherwise, if $|\Delta i_{as}| < h$, the inverter lag retains its current conduction mode. The hysteresis band in effect regulates

the maximum current ripple in phase-a. The operation of the other two hysteresis controllers can be similarly described.

Based on the conduction modes tabulated in Table II, the two - axis stator voltages V_{ds} and V_{qs}, in closed loop fashion, can be expressed as function of Ns and inverter dc input voltage Vc.

$$V_{ds} = \frac{2}{3}\text{Cos}\left[\theta r + (2 - Ns)\frac{\pi}{3}\right]\text{Vc.FW} \quad \text{.....(3.15)}$$

$$V_{qs} = \frac{2}{3}\text{Sin}\left[\theta r + (2 - Ns)\frac{\pi}{3}\right]\text{Vc.FW} \quad \text{.....(3.16)}$$

Where V_{ds} and V_{qs} serve as input to (3.12) and (3.13)

In this chapter the proposed scheme of speed control of permanent magnet synchronous motor drive is described in detail. The mathematical modeling of permanent magnet synchronous machine and controllers are also given.

CHAPTER – 4

SIMULATION OF PERMANENT MAGNET SYNCHRONOUS MOTOR DRIVE

In order to validate the control strategy of PMSM drive, simulation studies were made using a software in C language according to the algorithm given in the form of flow charts in Fig 4.1. The basic structure of this simulated drive system in shown in Fig (3.1) and details of PMSM used for simulation is given in Appendix B. The mathmatical models of PMSM and controllers are given in previous chapter, which are required for simulation purpose.

The nonlinear model of the PMSM given by equations (3.11)-(3.13) is

$$pw_r = (T_e - T_L - Bw_r)/J_m$$

$$pi_{ds} = (V_{ds} - r_1 i_{ds} + w_s L_q i_{qs})/L_d$$

$$pi_{qs} = (V_{qs} - r_1 i_{qs} + w_s L_d i_{ds} - w_s \lambda a_f)/L_q$$

These equation represent three state (w_r, i_{ds}, i_{qs}) nonlinear differential equations, these are used in the numerical simulation.

To achieve the required control approach, the digital speed control in Fig. (3.1). The system is assumed to be operate under a uniform sampling rate. In each sampling period, the deviation between the reference speed w_r^* and the feedback motor speed w_r is processed by a digital PI control algorithm that generates the torque command Te*

Let $\Delta w_r = w_r^* - w_r$.

$$\frac{T_e^*(z)}{\Delta w_r(z)} = K_p + \frac{Ki}{(1 - Z^{-1})}$$

taking the inverse z - transform of (3.14)

$$T_e^*(kT) = K_p \Delta w_r(kT) + Ki \sum_{i=0}^{k} \Delta w_r(iT) \quad \text{.....(4.1)}$$

for k = 1,2.....

where T is the sampling period.

Define a new variable

$$\alpha(kT) = \sum_{i=0}^{k} \Delta w_r(iT)$$

Where $\Delta w_r(0) = 0$

Equation (4.1) can be rewritten as

$$T_e^*(kT) = K_p \Delta w_r(kT) + Ki\alpha(kT) \quad \text{.....(4.2)}$$

and $\alpha(0) = 0$

This T_e^* (kT) is passed through a limiter to form the magnitude i_s^* of the stator current vector. i_s^* and T_e^* are related by

$$i_s^* = \begin{cases} T_e^*, \max & T_e^* \geq T_e^*, \max \\ T_e^* & -T_e^*, \max \leq T_e^* \leq T_e^*, \max \\ -T_e^*, \max & T_e^* \leq T_e^*, \max \end{cases} \qquad (4.3)$$

In order to accurately identify the position of the stator current vector in the d-q coordinate frame, the absolute rotor position and the angle must be determined. The absolute rotor position is measured by using the resolver mounted on the motor shaft and the RDC. The d-axis and the rotor flux positions are determined accordingly, since they all align with the absolute rotor position. The angle is computed via the three phase to two phase transformation of the stator line currents. Let i_{as}, i_{bs} and i_{cs} be the three phase stator line currents that are obtained by using current sensors. The two axis stator currents i_{ds} and i_{qs} are computed

$$\begin{bmatrix} i_{ds} \\ i_{qs} \\ 0 \end{bmatrix} = \frac{2}{3} \begin{bmatrix} \mathrm{Cos}\theta r & \mathrm{Cos}(\theta r - \frac{2\pi}{3}) & \mathrm{Cos}(\theta r + \frac{2\pi}{3}) \\ \mathrm{Sin}\theta r & \mathrm{Sin}(\theta r - \frac{2\pi}{3}) & \mathrm{Sin}(\theta r + \frac{2\pi}{3}) \\ \frac{1}{2} & \frac{1}{2} & \frac{1}{2} \end{bmatrix} \begin{bmatrix} i_{as} \\ i_{bs} \\ i_{cs} \end{bmatrix}$$

Where θ_r is the absolute rotor position.

The angle $\xi = \tan^{-1}(i_{ds}/i_{qs})$

As mentioned before, the control objective is to position the stator current vector on the q axis so that $i_{ds} = 0$ (hence $\xi = 0$) and torque per ampere may be achieved. Referring to Fig. 3.2 through the feedback, computation of the stator current vector is assumed to be at the shown position i.e, i_s lags the q-axis by an angle ξ. If the stator current vector is to be located on the q-axis during the next sampling period, the generated stator current command vector must lead the q-axis by an angle ξ. Thus, the generated three-phase current commands are given by

$$
\begin{aligned}
i_{as}^* &= i_s^* \, \mathrm{Sin}(\theta_r + \xi^*) \\
i_{bs}^* &= i_s^* \, \mathrm{Sin}(\theta_r - \frac{2\pi}{3} + \xi^*) \\
i_{cs}^* &= i_s^* \, \mathrm{Sin}(\theta_r + \frac{2\pi}{3} + \xi^*)
\end{aligned}
\qquad (4.5)
$$

Where i_s^* is computed from (4.3)

$\xi^* = \tan^{-1}\left(\frac{-i_{ds}}{i_{qs}}\right)$ if i_s lags the q axis

and $\xi = 0$, if i_s leads the q-axis.

The generated three phase line current commands as computed from eq. (4.5) serve as references for the current hysteresis controlled PWM VSI.

The deviation in the currnet is

$$\Delta i_{as} = i_{as}^{*} - i_{as}$$

$$\Delta i_{bs} = i_{bs}^{*} - i_{bs}$$

$$\Delta i_{cs} = i_{cs}^{*} - i_{cs}$$

Based on the conduction modes tabulated in Table II, the two axis stator voltages V_{ds} and V_{qs}, in closed loop fashion can be expressed as a function of Ns and inverter dc input Vc given in eq. (3.15) and (3.16). are

$$V_{ds} = \frac{2}{3}\mathrm{Cos}\left[\theta r + (2 - Ns)\frac{\pi}{3}\right]\mathrm{Vc.FW}$$

$$V_{qs} = \frac{2}{3}\mathrm{Sin}\left[\theta r + (2 - Ns)\frac{\pi}{3}\right]\mathrm{Vc.FW}$$

these V_{ds} V_{qs} serve as input to (3.12) and (3.13).

LOW SPEED OPERATION

One drawback of the hysteresis controller is that for very low speed operation, the three phase current errors Δi_{as}, Δi_{bs}, and Δi_{cs} are very small and lie within the hysteresis band. This leads to the conduction modes of free-wheeling periods. All the three inverter legs are either turned ON or OFF. The machine is disconnected from the inverter power supply. This

results in insufficient torque for motion control. Thus, the performance of the current hysteresis controllers is degraded during very low speed operation.

To improve the low speed operation of the motor drive some modifications of the hysteresis controllers have been proposed. We choose the method of controlling the duration of the free wheeling period. When the free wheeling period is detected, it is allowed to continue for a certain duration (e.g. 100 uses). Then the hysteresis band h is set to zero for specified duration (e.g. 50 sec.) of free wheeling period in a periodic fashion. This approach not only eliminates free wheeling periods but also provides protection for devices through delay switching that avoids excessive modulation. The lookout circuit shown in fig. (3.4) is used to delay the switching of transistors, thus reducing the modulation frequency and losses.

4.1 ALGORITHM AND FLOW CHART

The simulation procedure is summarized as follows:

Step 1 : Set the input speed command wr*, the hysteresis band h, the sampling period T, the number of iteration N and the duration of free wheeling period τ.

Step 2 : Determine the initial values for the state variables of the motor level equation.

Set the integration step size δ.

Let n = 1 and i = 0

Step 3: For n = 1,2, ...if n=1 .or n. δ = a multiple of T. Compute Te* by

$$T_e^*(kT) = k_p \Delta w_r(kT) + Ki\alpha(kT)$$

and the angle ξ^* from

$$\xi^* = \tan^{-1}\left(\frac{-i_{ds}}{i_{qs}}\right)$$

for n = 1, $\xi^* = 0$

otherwise, retain the values of Te* and ξ^* obtained at the $(n-1)^{th}$ iteration.

Step 4: Compute i_s^* from

$$i_s^* = \begin{cases} T_e^{*,max} & T_e^* \geq T_e^{*,max} \\ T_e^* & -T_e^{*,max} \leq T_e^* \leq T_e^{*,max} \\ -T_e^{*,max} & T_e^* \leq T_e^{*,max} \end{cases}$$

Step 5: Compute i_{as}^*, i_{bs}^* and i_{cs}^* from

$$i_{as}^* = i_s^* \, \mathrm{Sin}(\theta_r + \xi^*)$$

$$i_{bs}^* = i_s^* \, \mathrm{Sin}(\theta_r - \frac{2\pi}{3} + \xi^*)$$

$$i_{cs}^* = i_s^* \, \mathrm{Sin}(\theta_r + \frac{2\pi}{3} + \xi^*)$$

Step 6: Compute the current deviatons Δi_{as}, Δi_{bs} and Δi_{cs} from

$$\Delta i_{as} = i_{as}^* - i_{as}$$

$\Delta i_{bs} = i_{bs}^* - i_{bs}$

$\Delta i_{cs} = i_{cs}^* - i_{cs}$

For each phase, determine which inverter leg is to be switched by comparing the current deviations with hysteresis band h.

Step 7: Determine the conduction modes Ns and FW, of the VSI by Table II.

Step 8: If FW = 1, go to step 9, otherwise, Set i = i+1

If $i.\delta \neq \tau$, go to step 9, otherwise, $i.\delta = \tau$ and the system is in the low-speed operating range.

Set h = 0 then go to step 12.

Step 9: Compute V_{ds} and V_{qs} by

$$V_{ds} = \frac{2}{3}\mathrm{Cos}\left[\theta_r + (2 - Ns)\frac{\pi}{3}\right]V_c.\,FW$$

$$V_{qs} = \frac{2}{3}\mathrm{Sin}\left[\theta_r + (2 - Ns)\frac{\pi}{3}\right]V_c.\,Fw$$

Step 10: Solve wr, ids and iqs by using the Runge-Kutta routine.

$pw_r = (T_e - T_L - Bw_r)/J_m$

$pi_{ds} = (V_{ds} - r_1\, i_{ds} + w_s\, L_q\, i_{qs})/L_d$

$pi_{qs} = (V_{qs} - r_1 i_{qs} - w_s L_d\, i_{ds} - w_s \lambda_{af})/L_q$

Step 11: Set n = n+1

If n = N, go to step 16

Otherwise, go to step 3.

Step 12: Same as step 9.

Step 13: Same as step 10.

Step 14: Set n = n+1. If n = N, go to step 16, otherwise, go to step 15.

Step 15: Execute steps 3-7.

Step 16: Stop.

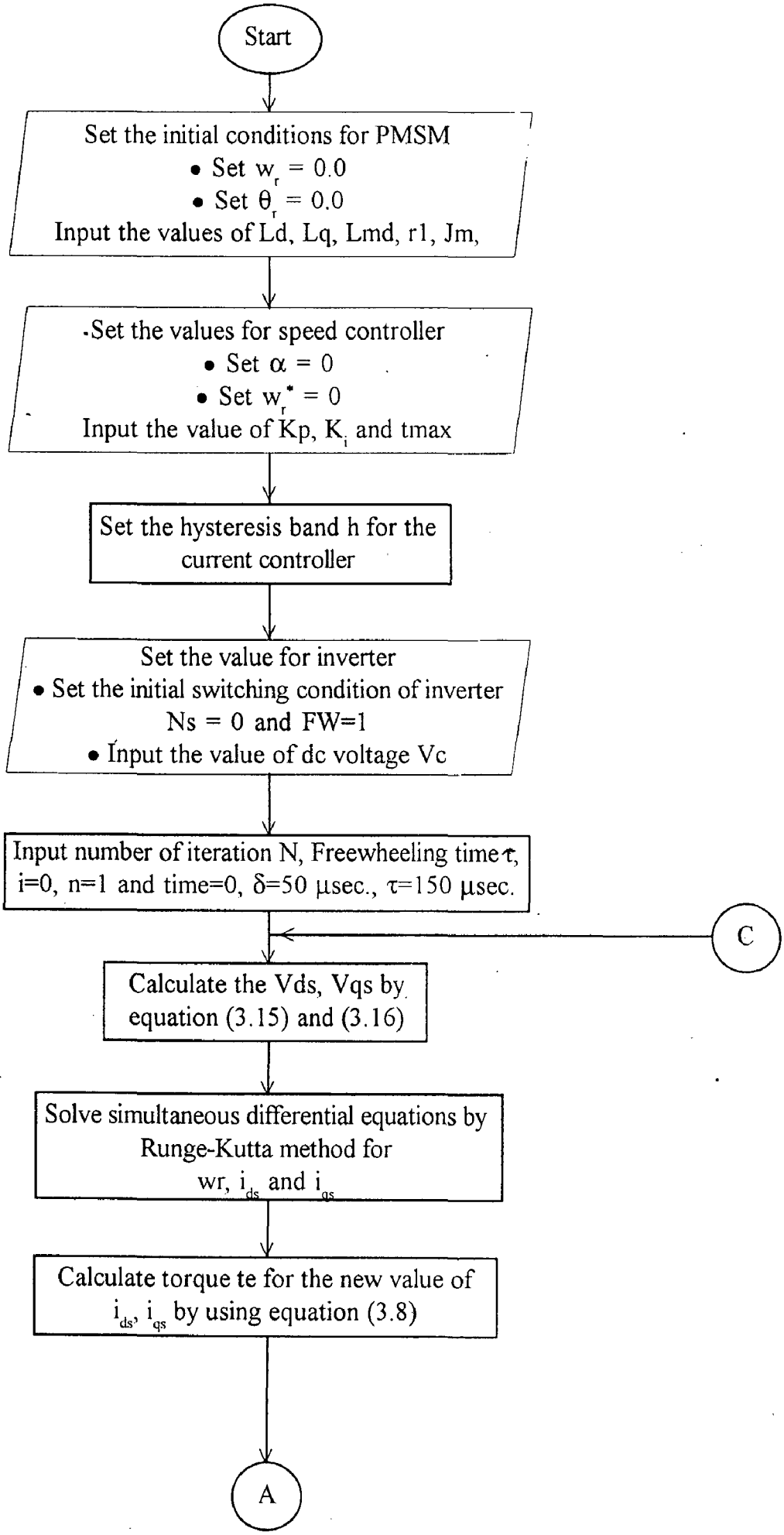
Start
Set the initial conditions for PMSM
• Set w_r = 0.0
• Set θ_r = 0.0
Input the values of Ld, Lq, Lmd, r1, Jm,
-Set the values for speed controller
• Set α = 0
• Set w_r^* = 0
Input the value of Kp, K_i and tmax
Set the hysteresis band h for the current controller
Set the value for inverter
• Set the initial switching condition of inverter Ns = 0 and FW=1
• Input the value of dc voltage Vc
Input number of iteration N, Freewheeling time τ, i=0, n=1 and time=0, δ=50 μsec., τ=150 μsec.
C
Calculate the Vds, Vqs by equation (3.15) and (3.16)
Solve simultaneous differential equations by Runge-Kutta method for wr, i_{ds} and i_{qs}
Calculate torque te for the new value of i_{ds}, i_{qs} by using equation (3.8)
A

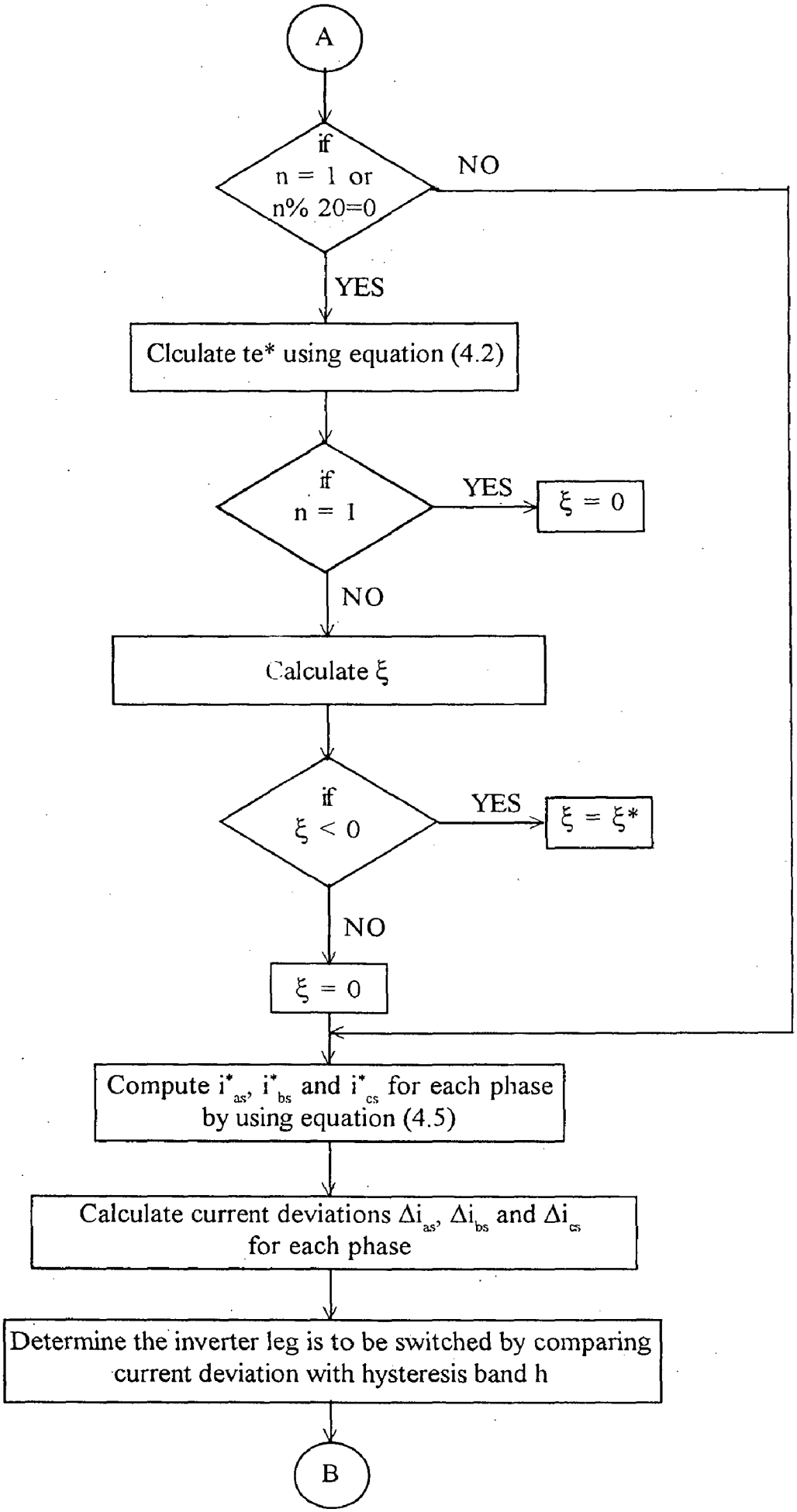
A
if
n = 1 or
n% 20=0
NO
YES
Clculate te* using equation (4.2)
if
n = 1
YES
ξ = 0
NO
Calculate ξ
if
ξ < 0
YES
ξ = ξ*
NO
ξ = 0
Compute i*as, i*bs and i*cs for each phase by using equation (4.5)
Calculate current deviations Δias, Δibs and Δics for each phase
Determine the inverter leg is to be switched by comparing current deviation with hysteresis band h
B

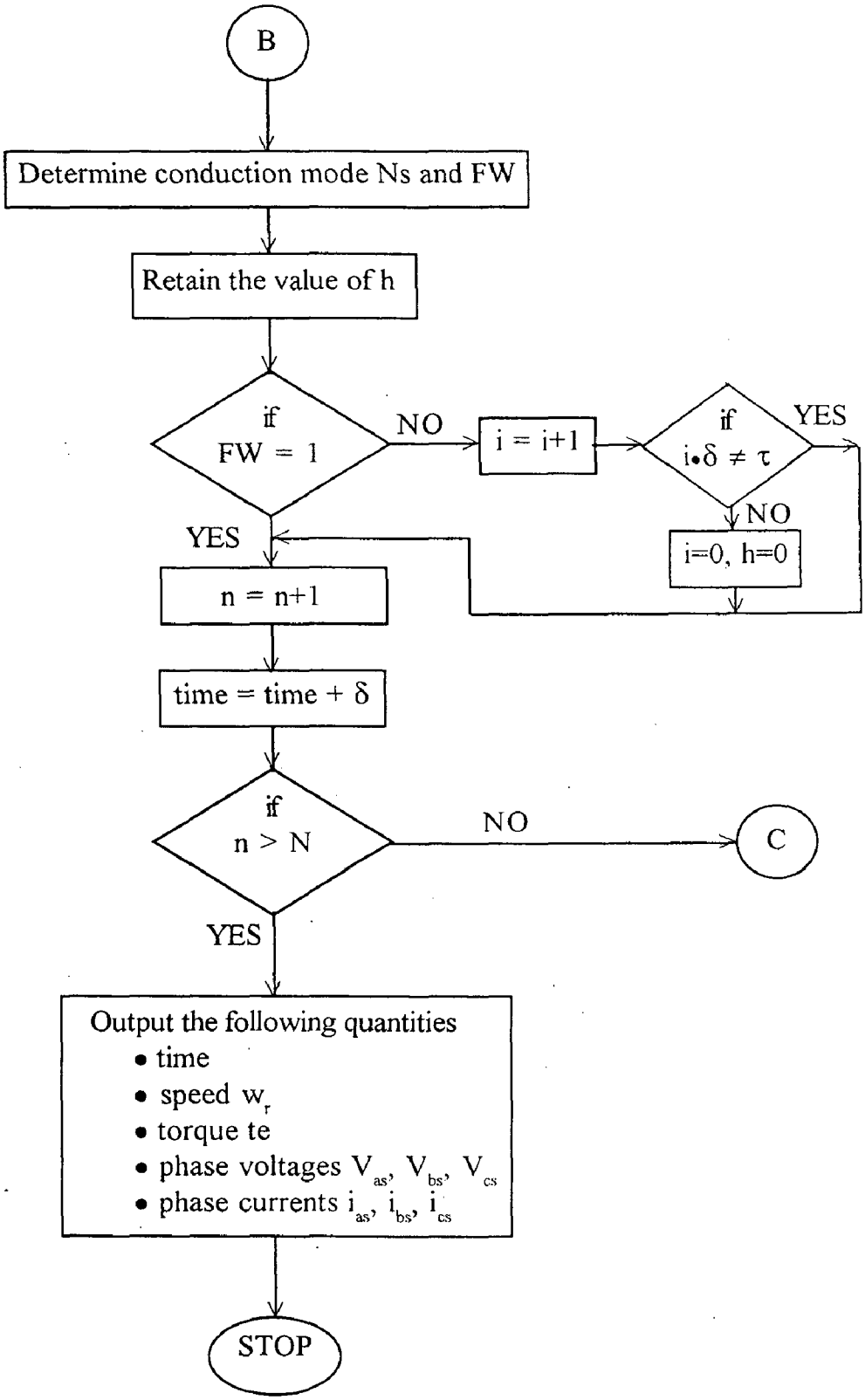

Fig. 4.1 : Flowchart of Software Simulation of PMSM Drive

4.2 DESIGN OF CONTROLLERS

4.2.1Design of Speed Controller

A PI controller is used as speed controller, Fig. (4.2) shows the simplified block diagrams of the speed controller.

In the z-domain, the linear transfer function in the feedforward loop is given by

$$G(z) = G_c(z)\, G_p(z)$$

$$G(z) = \frac{K_T T}{J_m} \frac{(K_p + K_i)z - K_p}{(z-1)^2} \quad \text{.....(4.6)}$$

The characteristics equation of the complete system can be written as

$$1 + G(z).1 = 0$$

$$(Z-1)^2 + \frac{K_T}{J_m}\left[(K_p + K_i)z - K_p\right] = 0 \quad \text{.....(4.7)}$$

$$(z^2 - 2Z+1) + A.K_p z + A\,Ki\,.Z - A\,K_p = 0$$

The above characteristic equation can be expressed in term of the controller parameters K_p and K_i as

$$K_p\, F_1(z) + K_i F_2(z) + F_3(z) = 0 \quad \text{.....(4.8)}$$

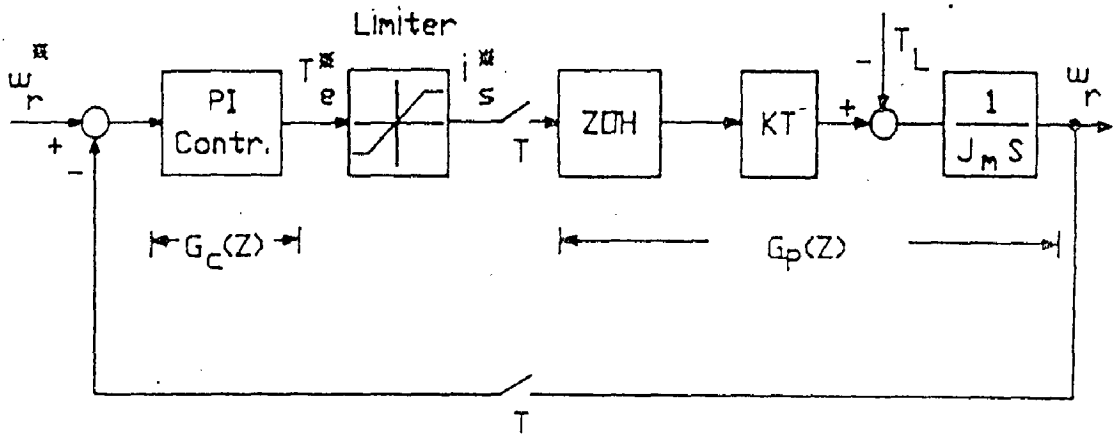

Fig. 4.2 Simplified speed control system block diagram.

Where $F_1(z) = A(z-1)$

$F_2(z) = Az$

$F_3(z) = z^2-2z + 1$

$$A = \frac{K_T.T}{J_m}$$

T = Sampling period

The D- partition technique is applied to characteristic equation (4.8) by replacing the value of $z = e^{ST}$.

Where $S = -\sigma + jw$

and $S = -\varsigma w + jw\sqrt{1-\varsigma^2}$

where σ is the relative stability and ζ is the damping ration. The stability contours are plotted for different values of damping ratio and relative stability. The probable stable zones are identified based on the rule of shading of the D- partition boundary. A point check is made for a set of controller parameters from the probable stable zone by frequency scanning technique. The D-pantition boundary and the contour obtained by frequency scanning technique are shown in fig (4.3), (4.4), (4.5).

It is seen that the probable stable boundary collapses as the values of relative stability σ and damping ratio increases as shown in Fig (4.3). The final selection of controller parameters is made by companing the

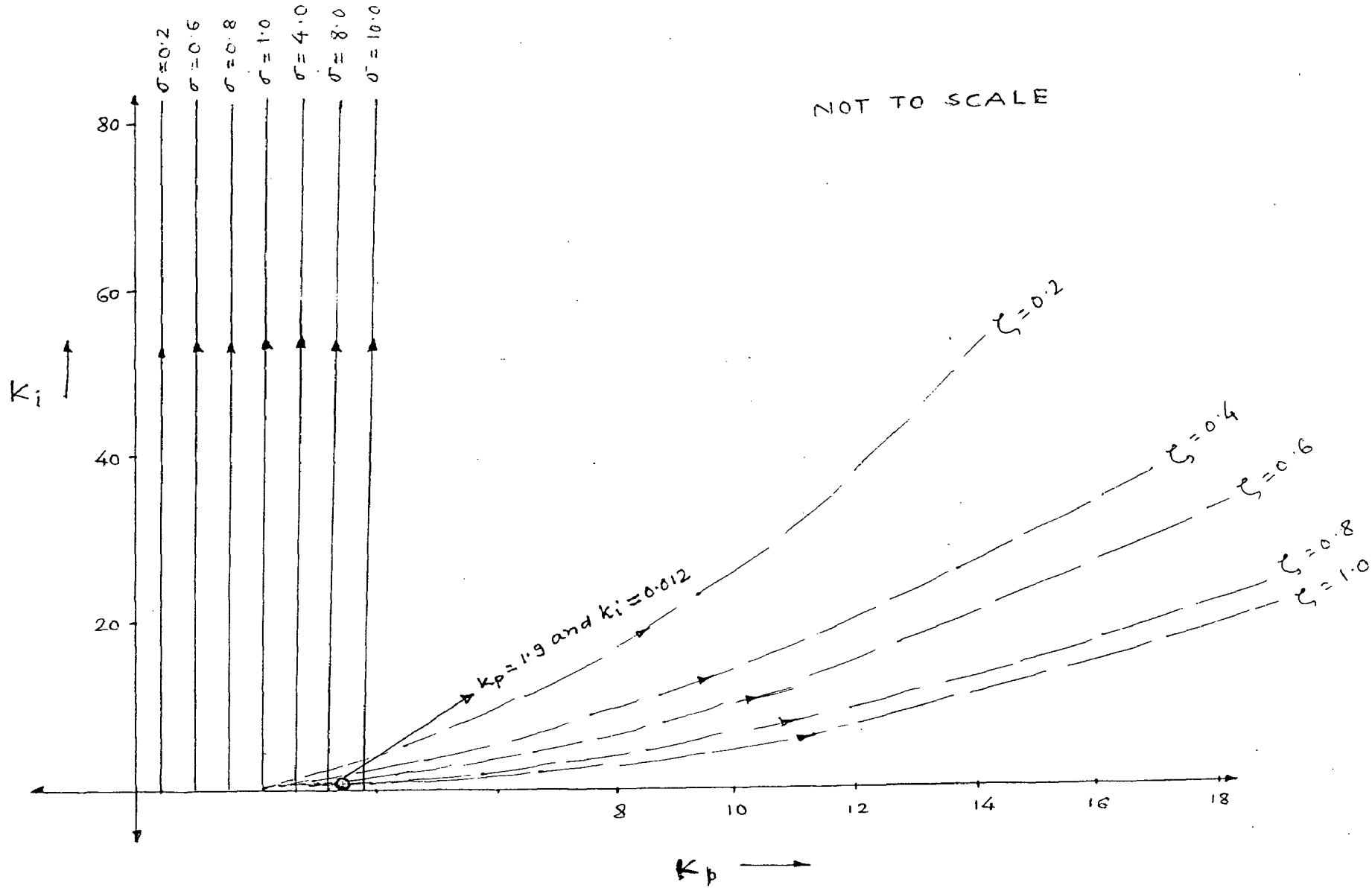

Fig. 4.3 D-Partition curve for speed controller with variation in σ and ξ

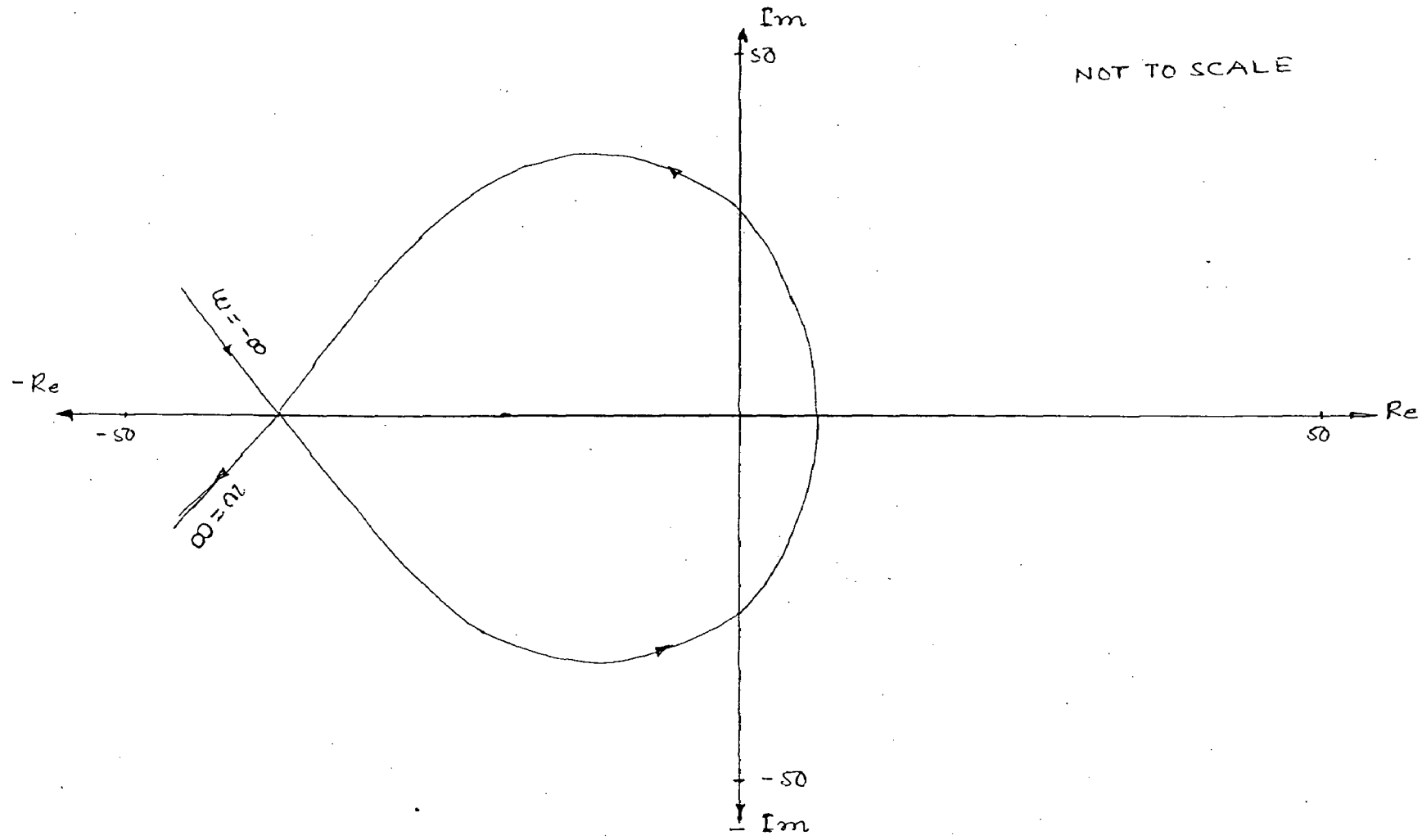

Fig. 4.4 Stability check for speed controller
(σ = 0.6 K_p = 1.9 and K = 0.012)

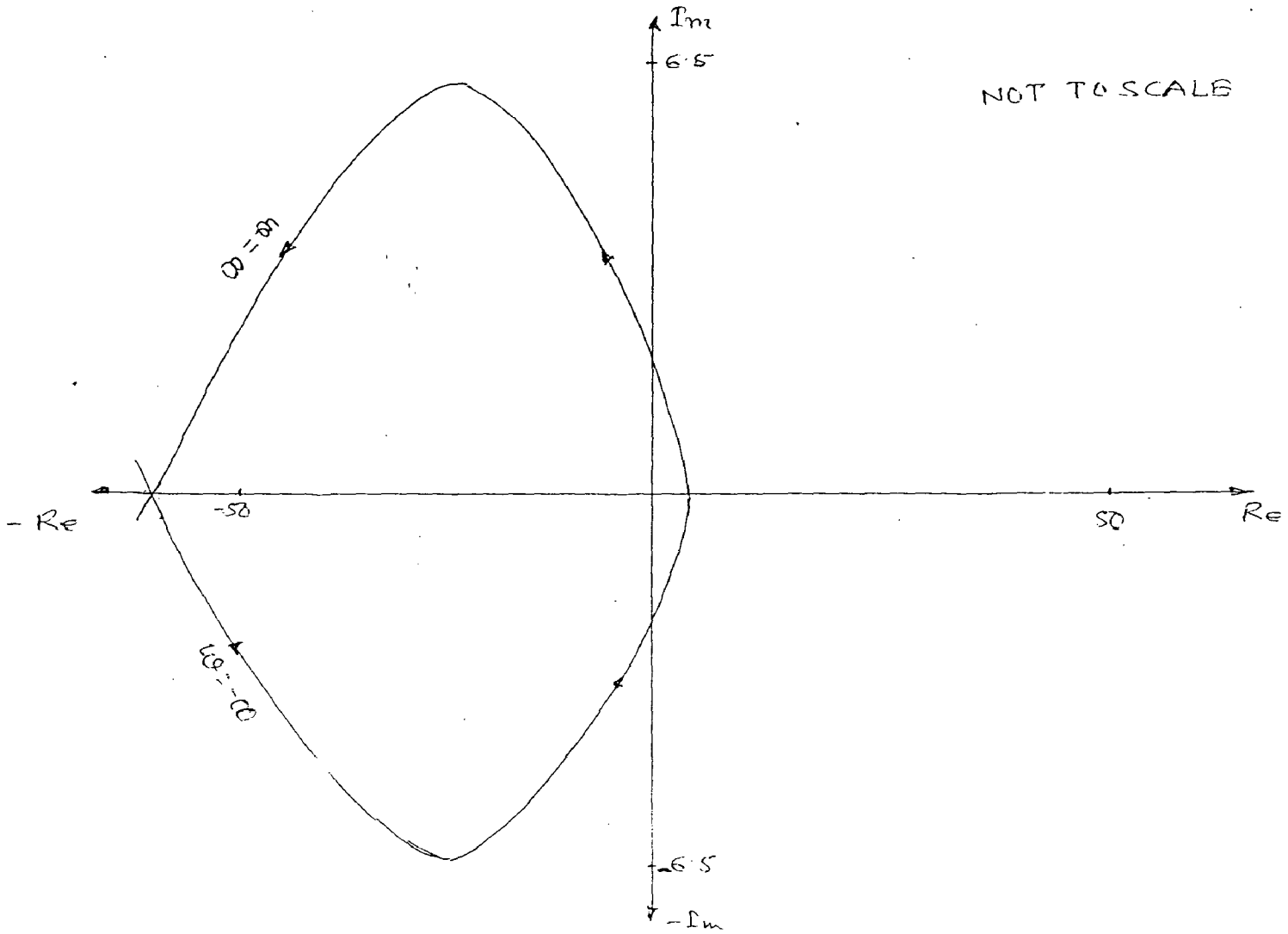

Fig. 4.5 Stability check for speed controller

(ξ = 0.9 K_p = 1.9 and K_i = 0.012)

response of drive for step change applied at different sets of controller parameters.

4.2.2Design of Current Controller

The principle employed in this control system is consists of controlling the inverter switches in such in way as to force the currents in the machine to follow references generated from a rotor position encoder. The current reference generator generates the three phase line current commands which serve as references. The three pairs of power switches provide eight conduction modes according to the switching of devices as decribed in detail in section 3.2.4

4.2.3 Transient Response of Drive System

At the various points selected from the probable stable area the response of the drive are plotted shown in fig (4.6), (4.7), (4.8), (4.9) & (4.10).

The maximum over-shoot and settling time for above responses are given in table III.

Table III

Figure No.	Kp	Ki	Maximum over-shoot (rad./sec.)	Settling Time (msec.)
4.6	12.0	1.0	81.0	90
4.7	8.0	0.4	71.0	130
4.8	3.0	0.06	60.5	195
4.9	2.3	0.0215	56.4	360
4.10	1.9	0.012	54.5	400

Visualizing the transient response of system with current controller the proper values of speed controller parameters are selected (i.e. Kp = 1.9 and Ki = 0.012)

In this chapter the complete algorithim and flow charts are given for the proposed speed control system. The parameter of the PI speed controller are designed on the basis of system stability and response of the system.

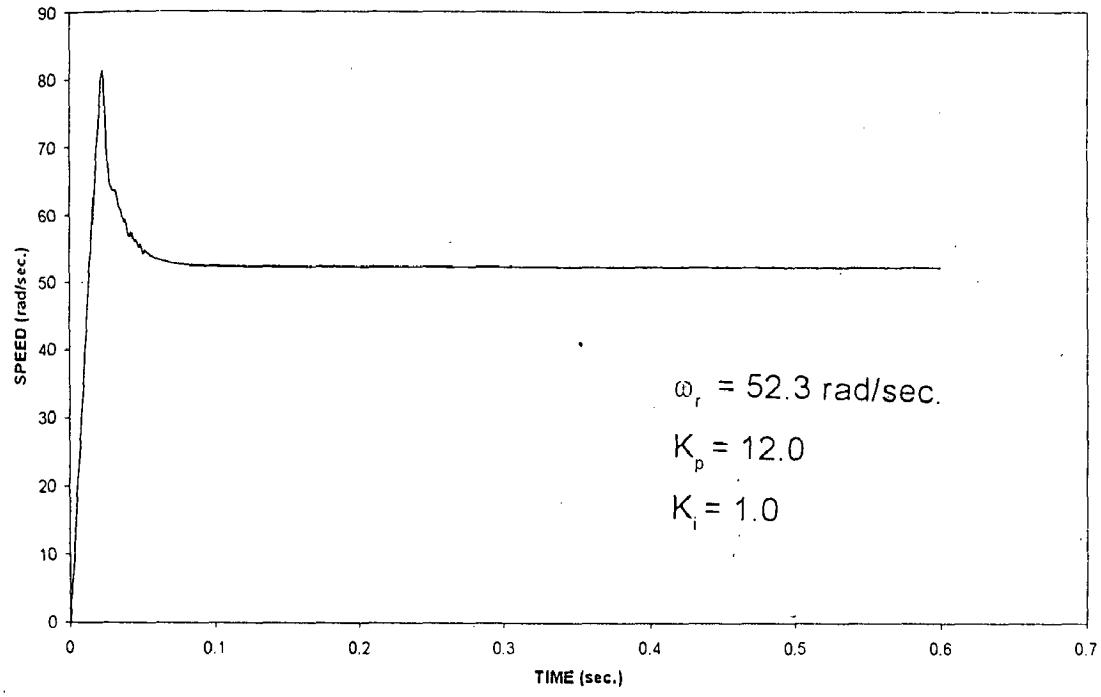

Fig.4.6 : SPEED Vs TIME

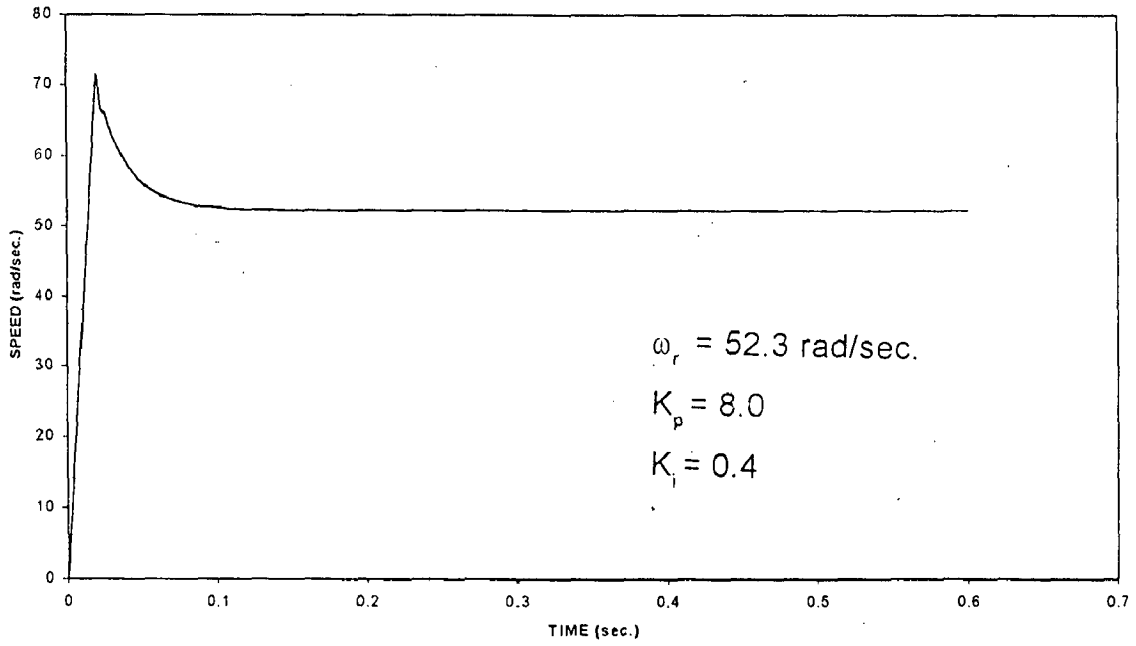

Fig.4.7 : SPEED Vs TIME

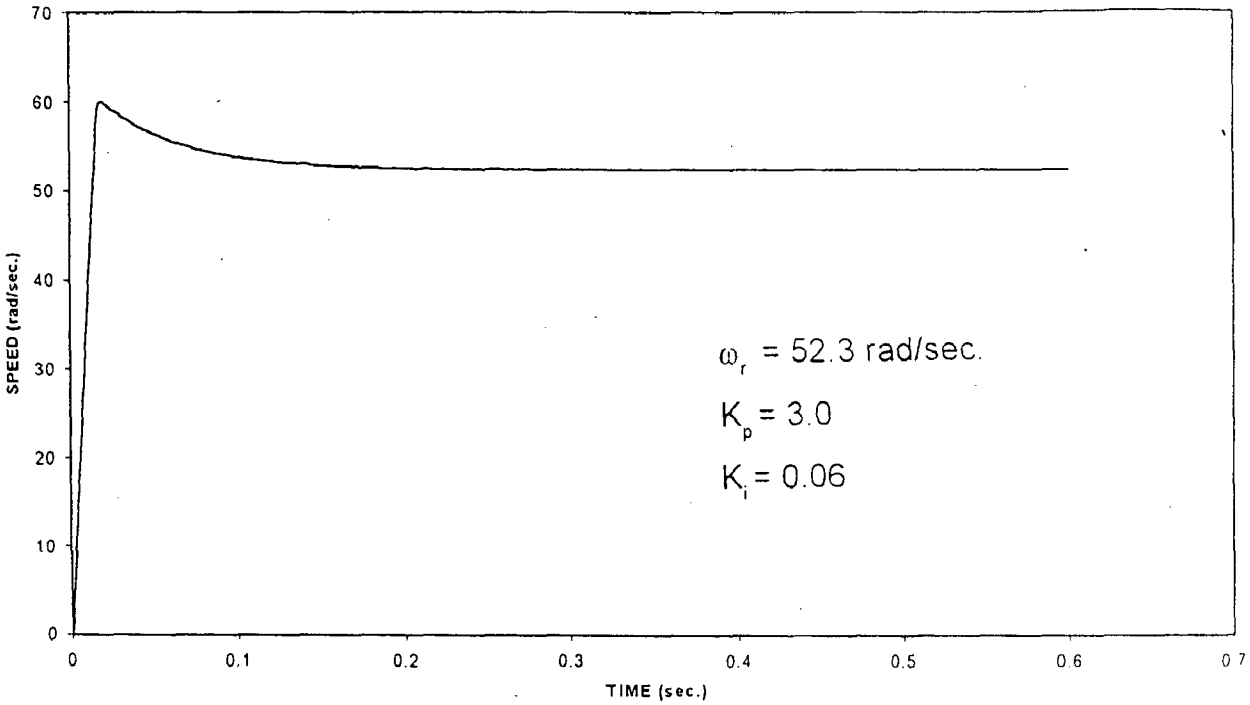

Fig.4.8 : SPEED Vs TIME

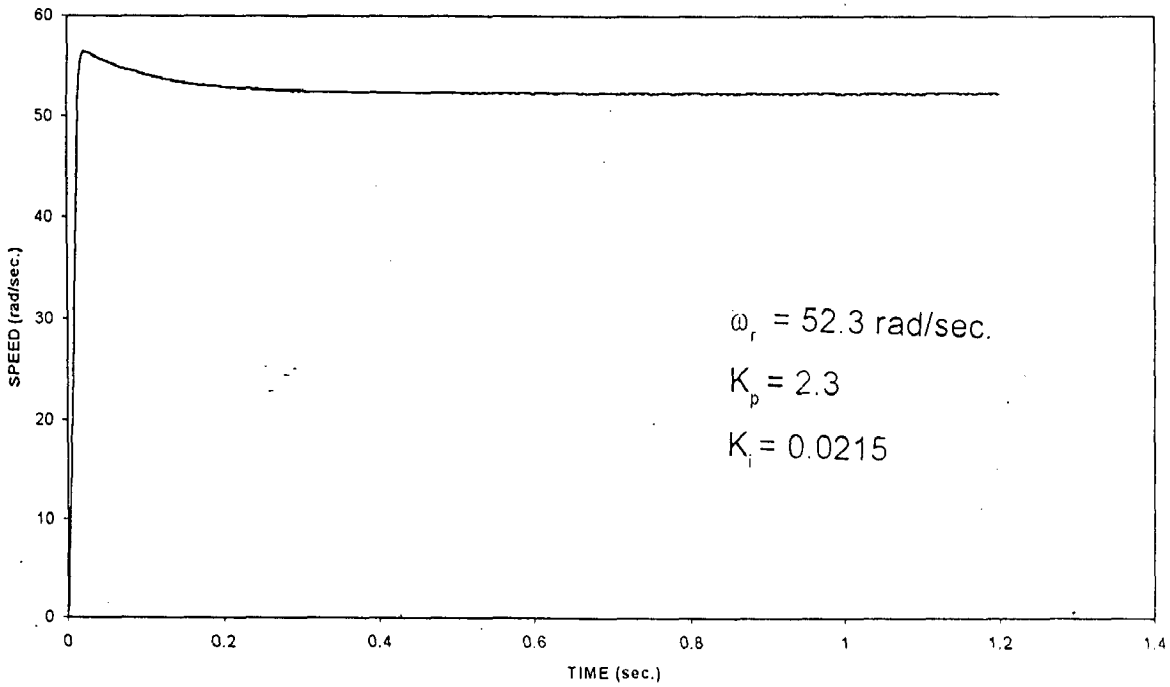

Fig.4.9 : SPEED Vs TIME

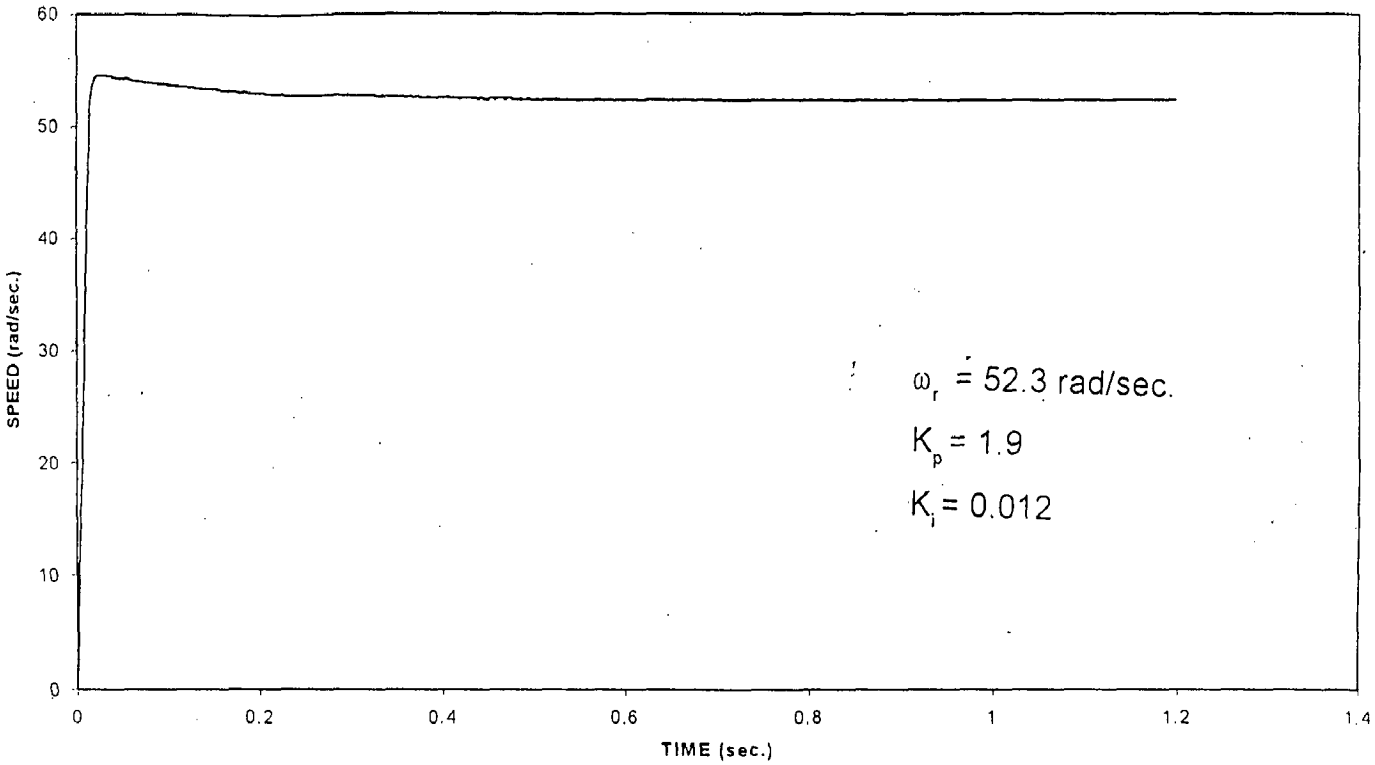

Fig.4.10: SPEED Vs TIME

CHAPTER-5

RESULTS AND DISCUSSION

In this chapter the simulated results of permanent magnet synchronous motor drive at different reference speeds and loads are presented and discussed in details as shown in Figs. 5.1. to 5.5.

Fig. 5.1(a) shows the transient and steady state response of the motor which is initially at rest and given a reference speed of 52.3 rad./sec. at no-load, the motor takes around 400 msec. as settling time. The torque versus time curve is shown in Fig. 5.1(b), during the startup period the commanded torque is taken higher than the rated torque this insures that the machine runs up in very short time. The motor torque is of pulsating nature, the motor torque pulsations are related linearly to the size of hysteresis band, larger the hysteresis band lower the inverter switching frequency and larger the motor torque pulsation. The stator phase current and stator phase voltage of phase-a are given in Fig. 5.1(c) and (d). The motor current goes to a very high value before settling down. The phase voltage is switched by hysteresis controller to keep the phase current within hysteresis band. Therefore phase current is approximately sinusoidal. Smaller the hysteresis band more close to the sine wave. Smaller hysteresis band, however, imply a high switching frequency, which is a practical limitation on the power switching capacity. The increased switching also implies increased inverter losses.

Fig. 5.2(a) and (b) show the speed and torque curves when machine is initially loaded with load, the reference speed is 52.3 rad/sec. and started rest. In this case machine takes more time to settle at reference speed (about 580 m.sec.), but the maximum overshoot is lesser. The torque at the switching instant reaches maximum value and when machine attain the maximum speed, it settle down at rated torque level, Fig. 5.2(c) and (d) show the corresponding phase-a current and voltage waveforms.

Fig. 5.3(a), (b), (c) and (d) show the speed, torque, phase current, and phase voltage respectively when the machine started at no load with reference speed 52.3 rad/sec., and at the time 0.9 sec. from starting the reference speed becomes 35.0 rad/sec. with sudden change in reference speed a fluctuation is produced in torque and current, here the new reference speed is lower than the running speed of the motor, so the torque and current becomes negative for a moment and then settle to their original value.

Curves in Fig. 5.4(a),(b),(c) and (d) show the speed, torque, phase current and phase voltage, when machine started at no-load with reference speed 52.3 rad/sec. As shown in figures the load is applied after 0.9 sec. from starting when machine is running under steady state. As the load is applied machine speed reduces for a moment and again it settles at reference speed. The machine settles at reference speed within 300 m. sec.

In next case, the machine is started from rest at no-load with reference speed 52.3 rad/sec. After 0.9 sec., the reference speed is reduced to 35 rad/sec. and with this new speed after 1.2 sec. load is applied. The respective speed,

torque, phase-a current and phase-a voltage are given in Fig. 5.5(a), (b), (c) and (d).

Simulation studies clearly show the better performance of PMSM drive system as machine settles down very quickly at the desired speed under various conditions of loading, with very small overshoot. Hence simulation results of PMSM drive system using current hysteresis controlled PWM voltage source inverter confirm the validity of proposed control technique.

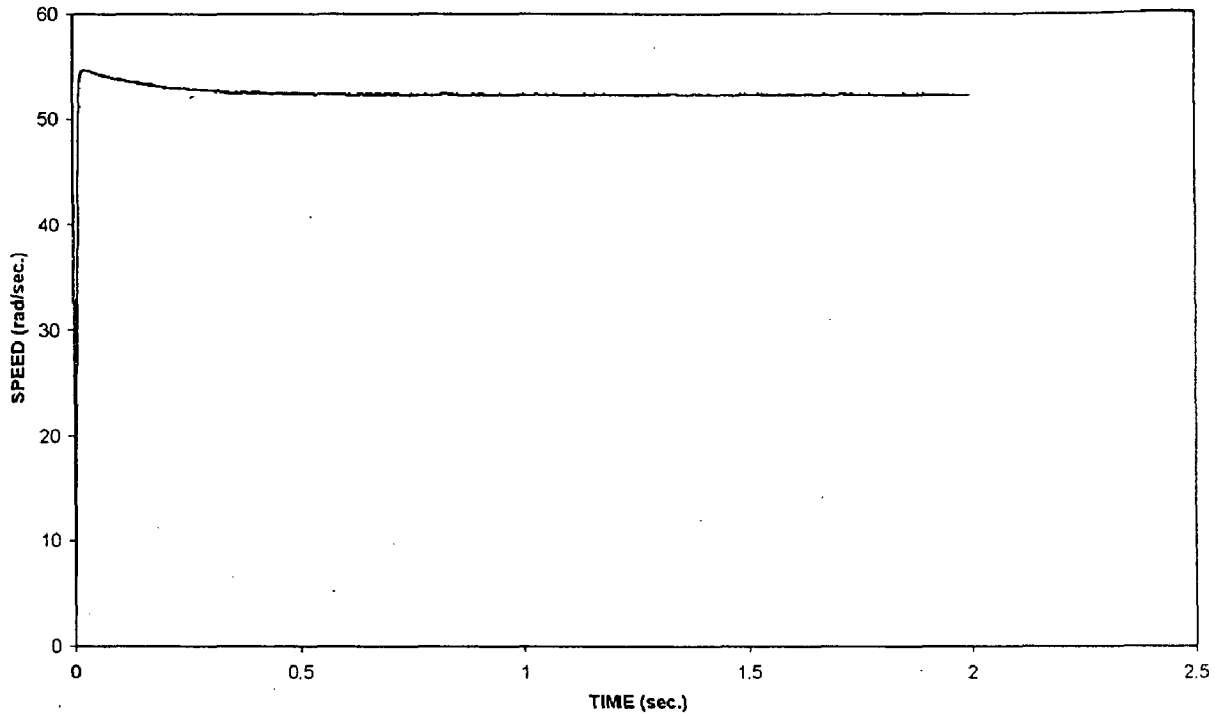

Fig.5.1(a) : SPEED Vs TIME

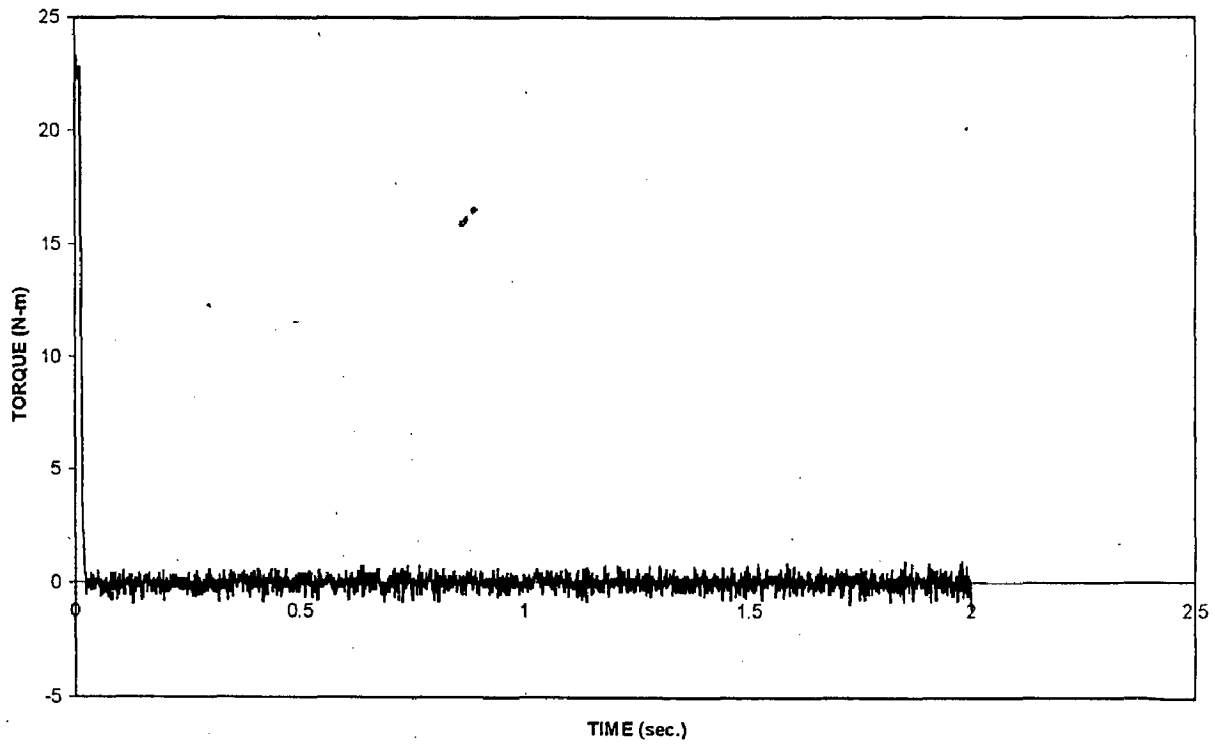

Fig.5.1(b) : TORQUE Vs TIME

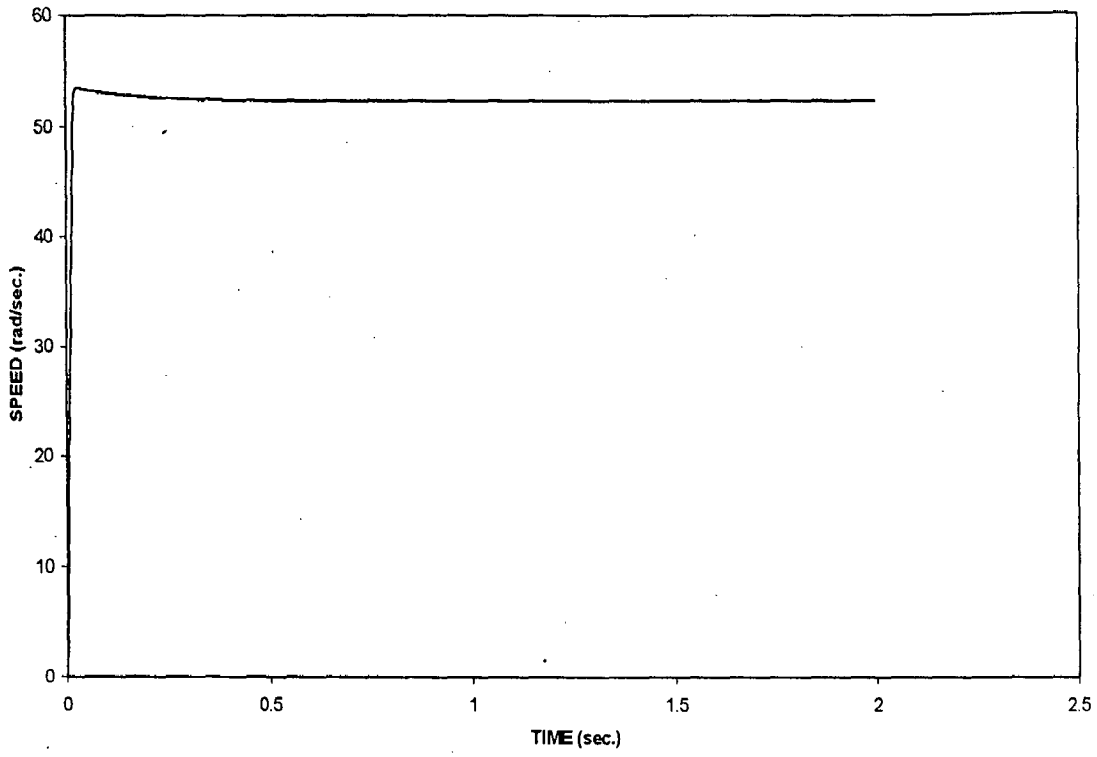

Fig.5.2(a) : SPEED Vs TIME

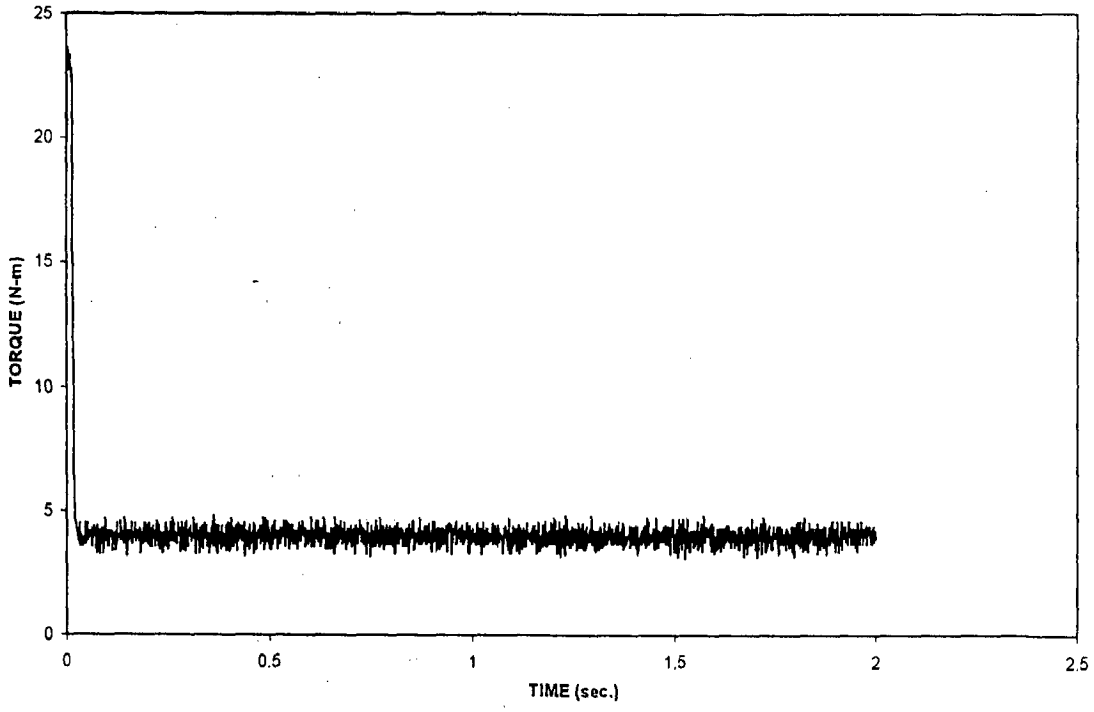

Fig.5.2(b) : TORQUE Vs TIME

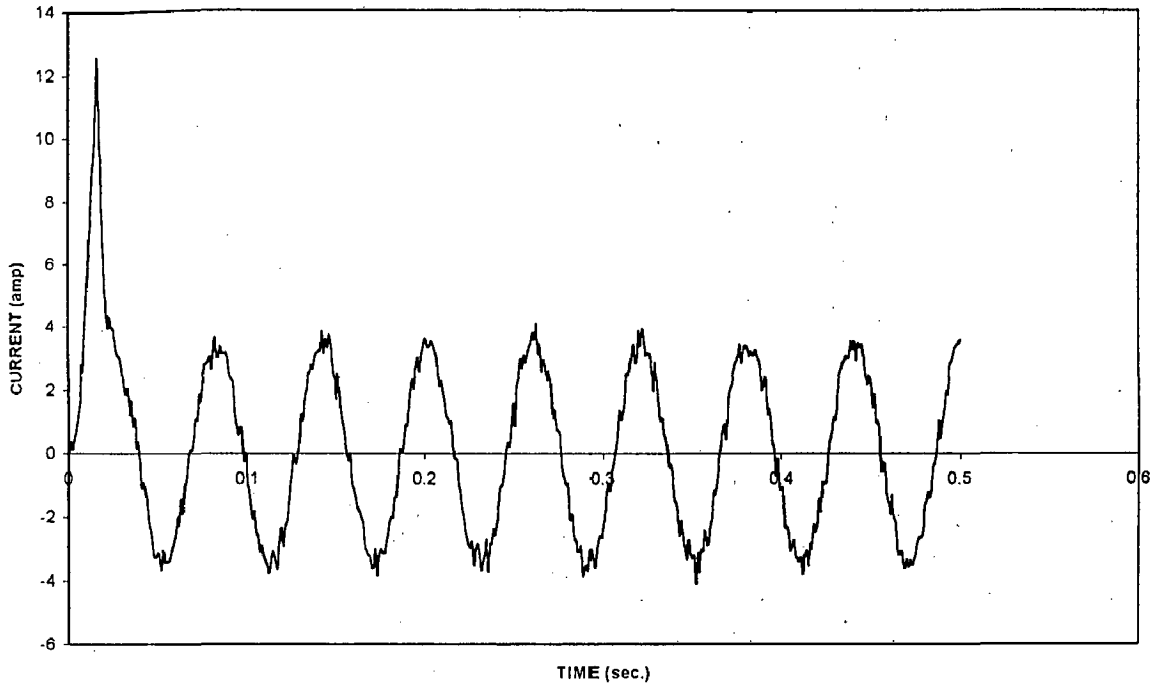

Fig.5.2(c) : STATOR CURRENT Vs TIME

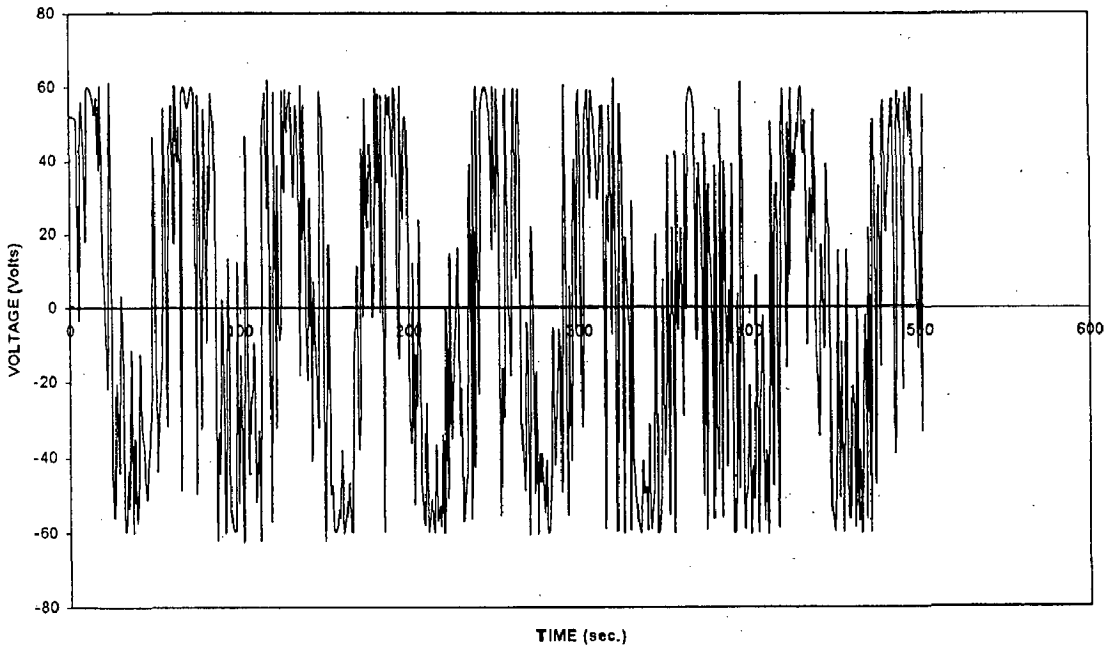

Fig.5.2(d) : STATOR VOLTAGE Vs TIME

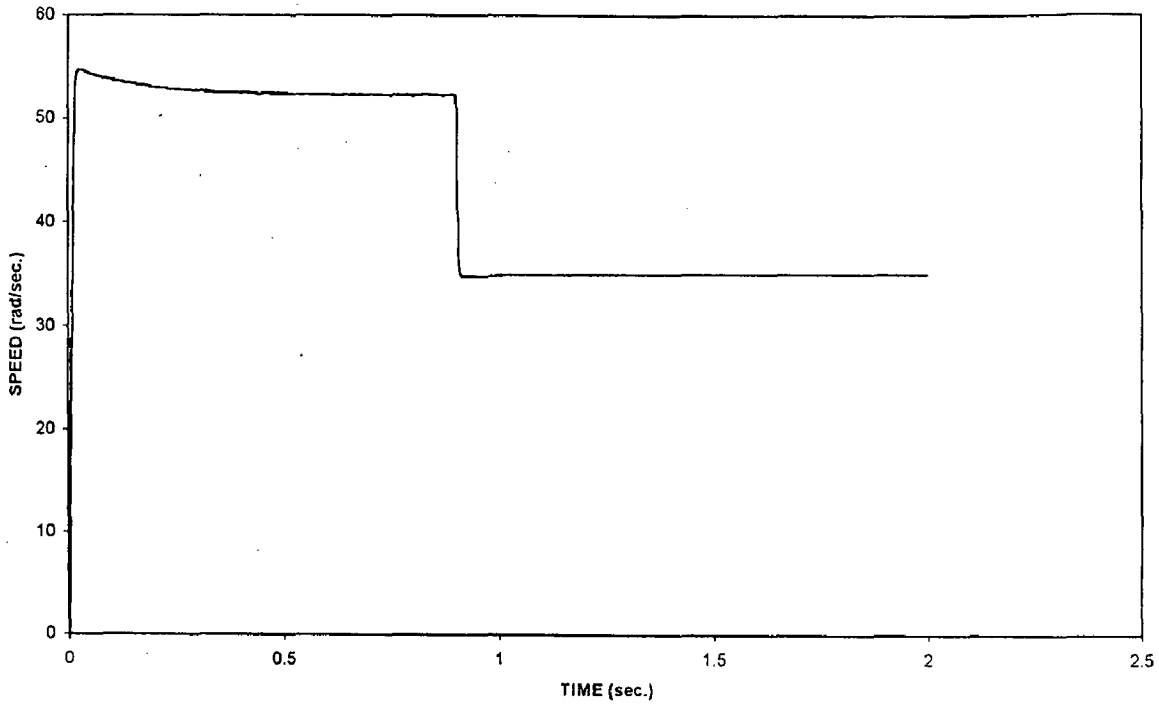

Fig.5.3(a) : SPEED Vs TIME

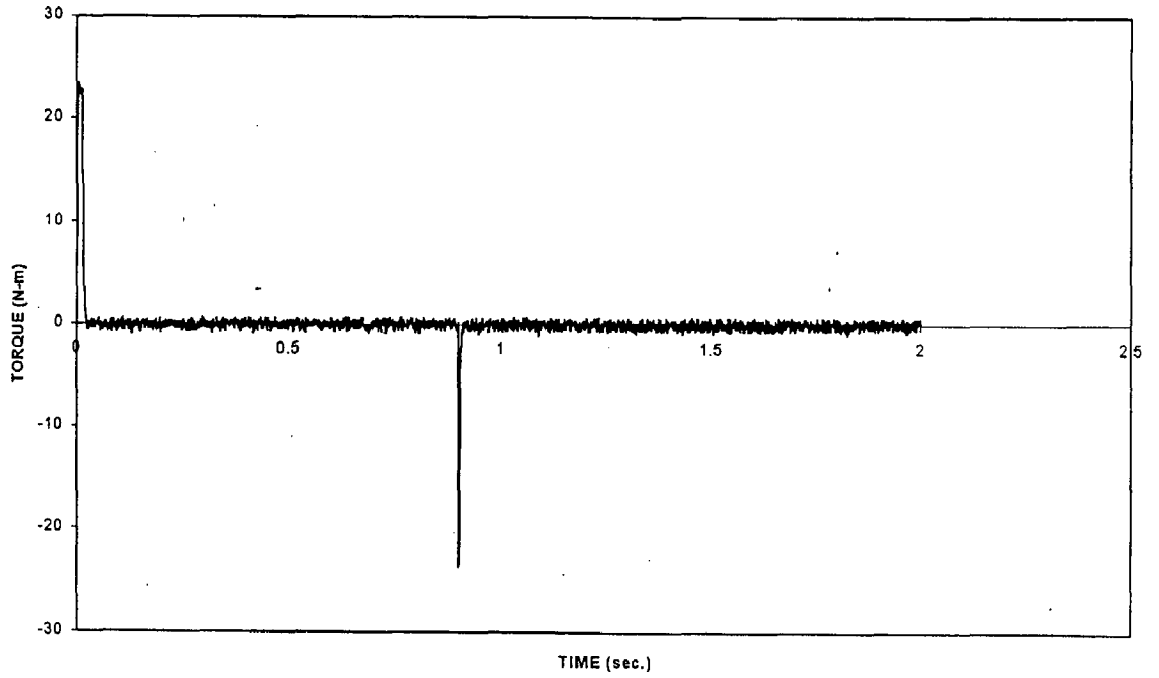

Fig.5.3(b) : TORQUE Vs TIME

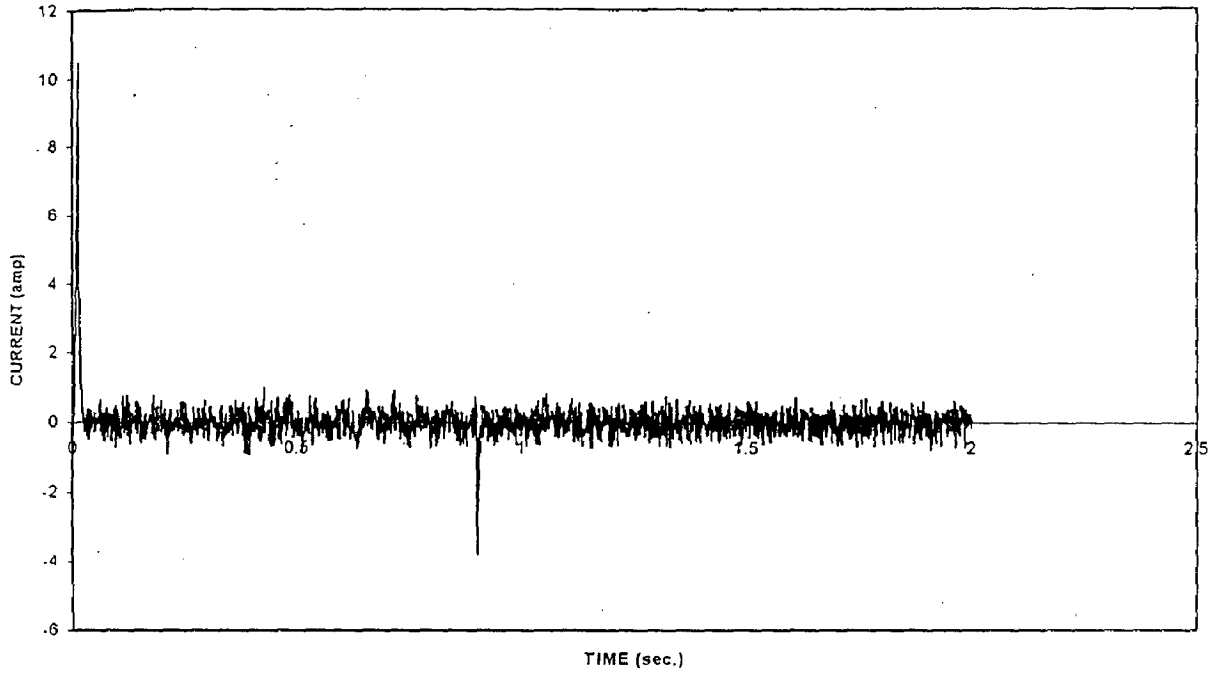

Fig.5.3(c) : STATOR PHASE CURRENT Vs TIME

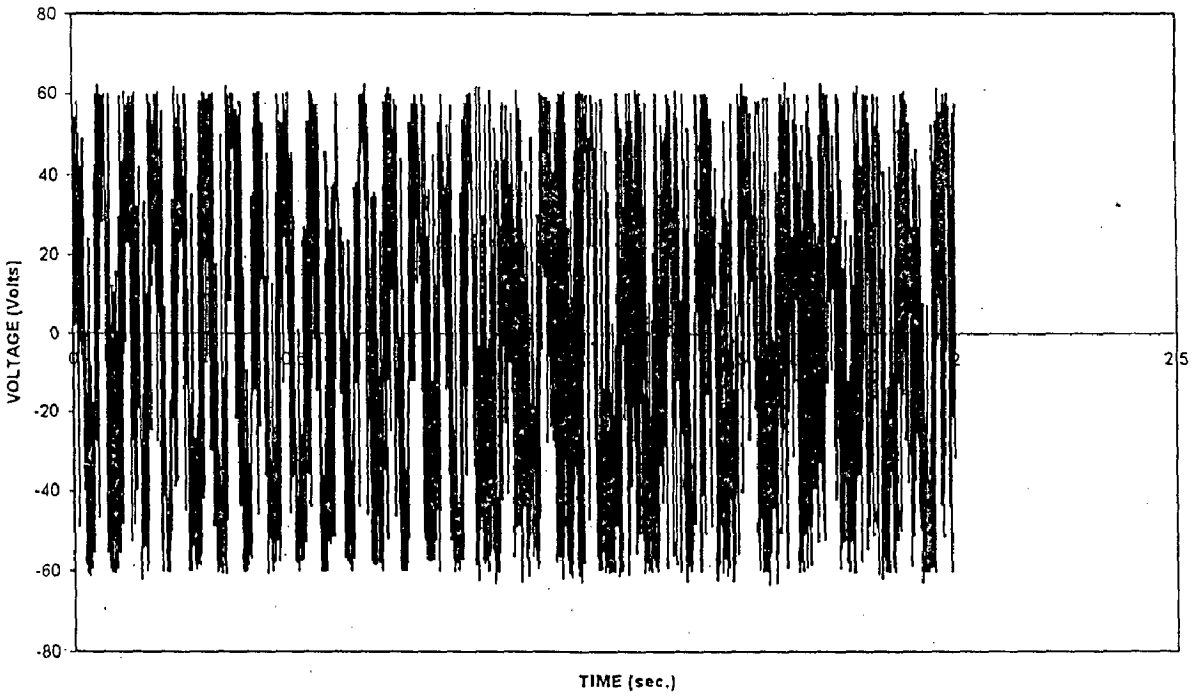

Fig.5.3(d) : STATOR PHASE VOLTAGE Vs TIME

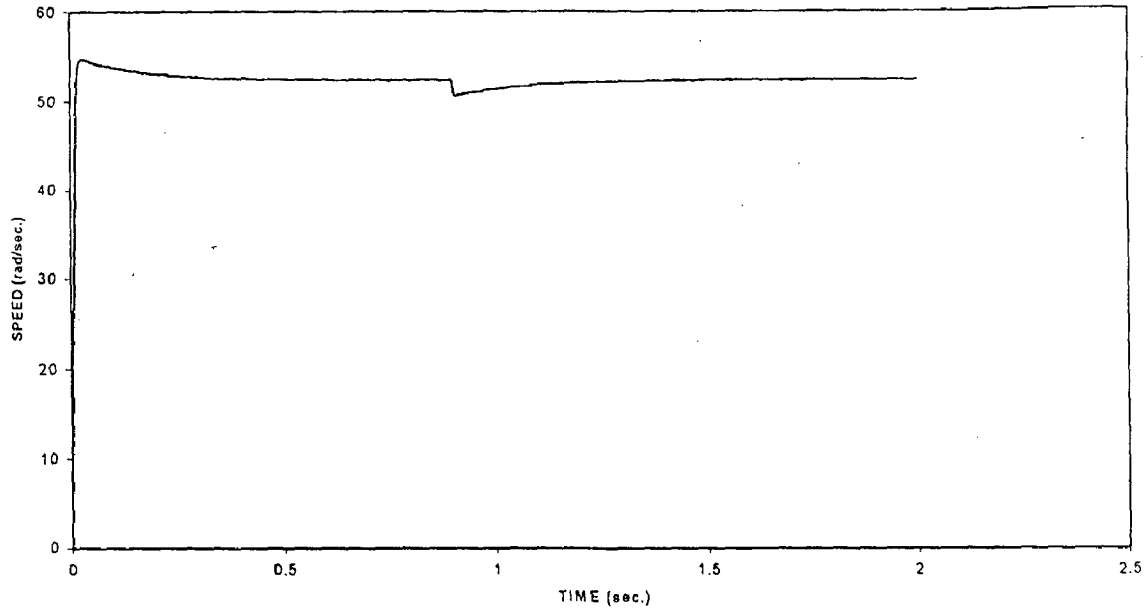

Fig.5.4(a) : SPEED Vs TIME

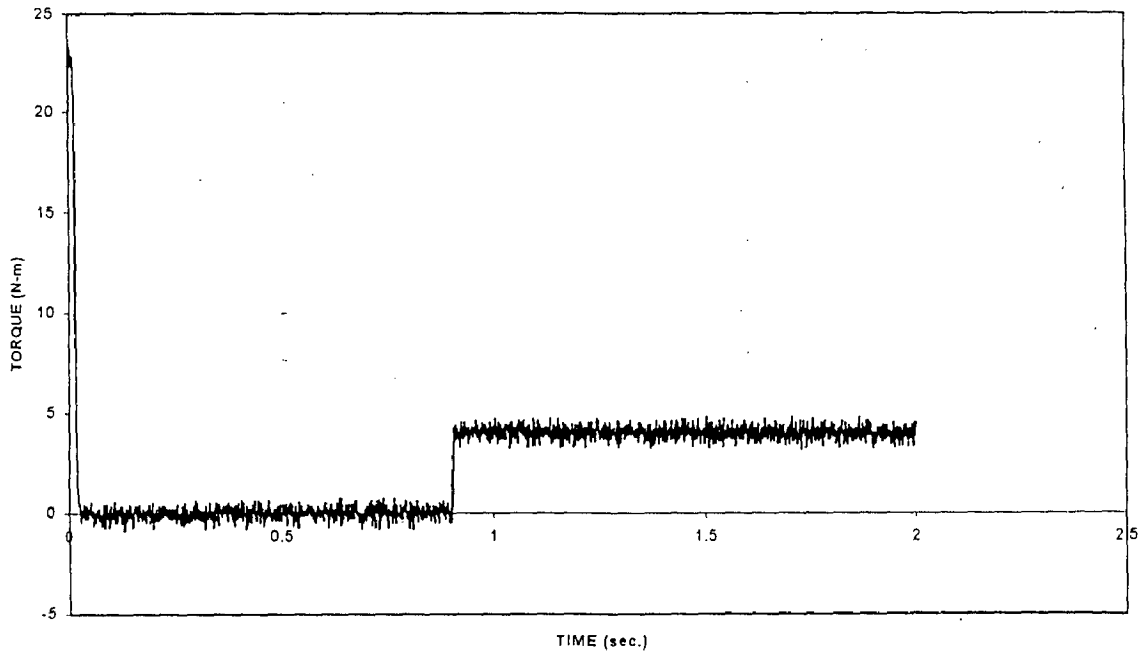

Fig.5.4(b) : TORQUE Vs TIME

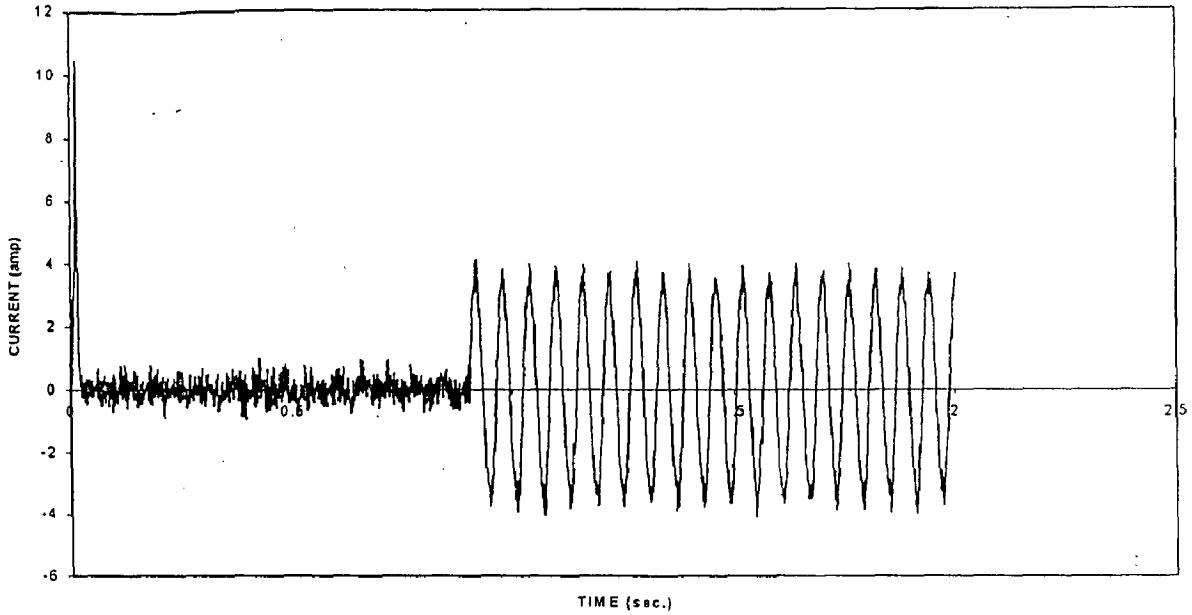

Fig.5.4(c) : STATOR PHASE CURRENT Vs TIME

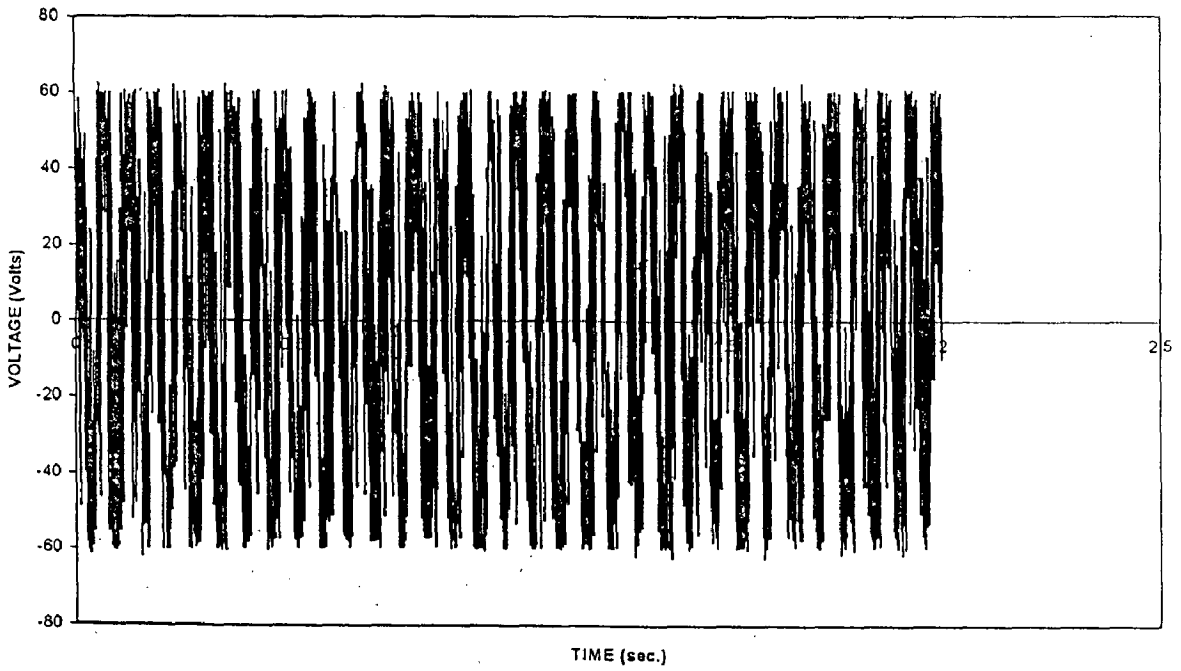

Fig.5.4(d) : STATOR PHASE VOLTAGE Vs TIME

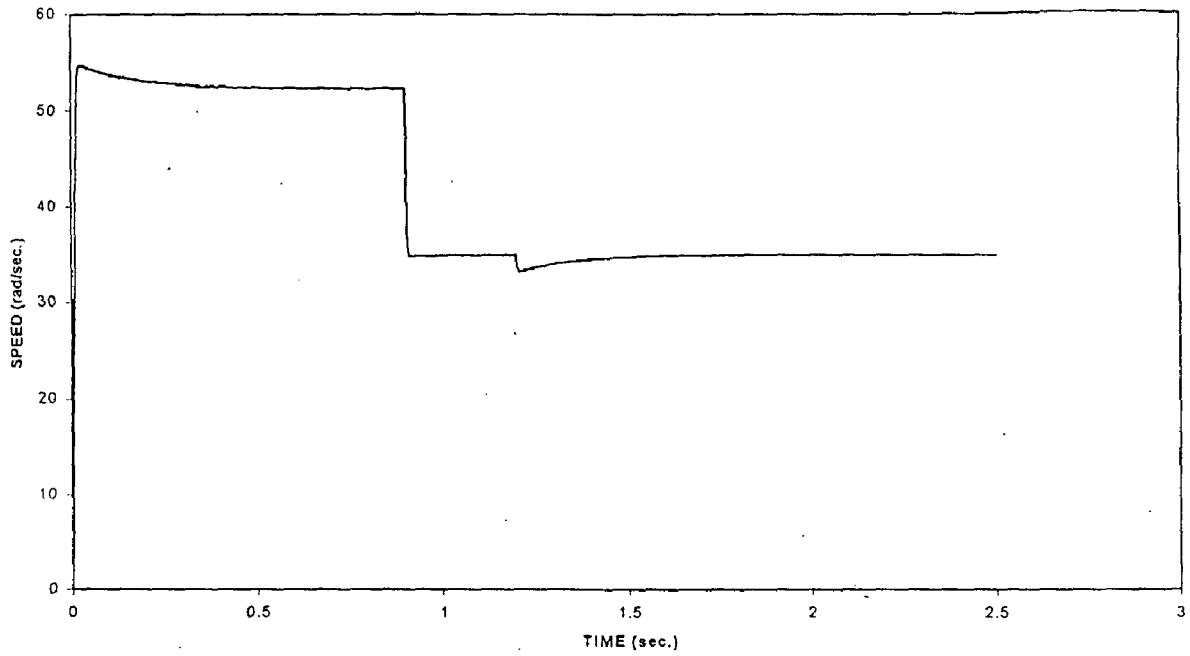

Fig.5.5(a) : SPEED Vs TIME

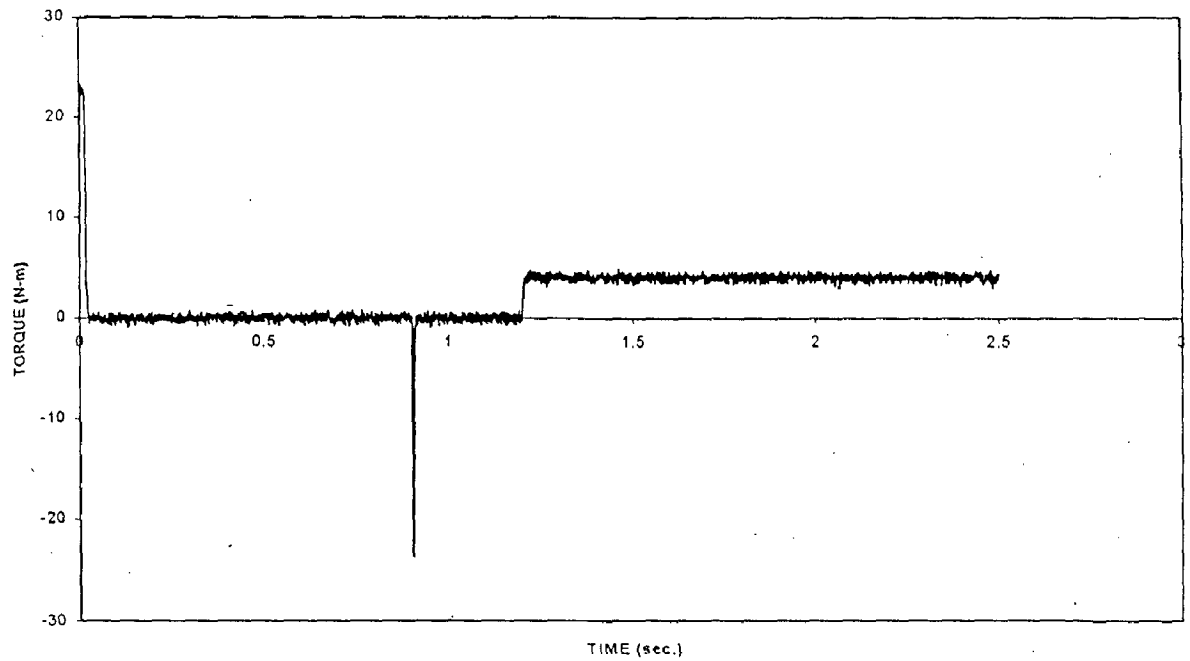

Fig.5.5(b) : TORQUE Vs TIME

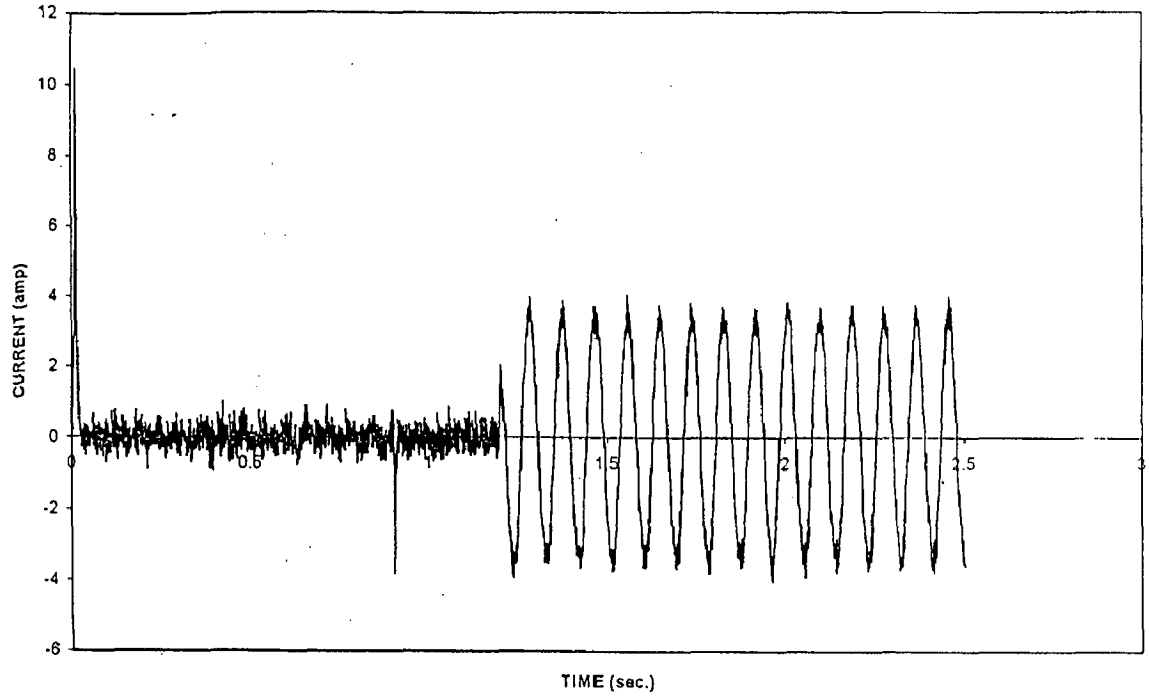

Fig.5.5(c) : STATOR PHASE CURRENT Vs TIME

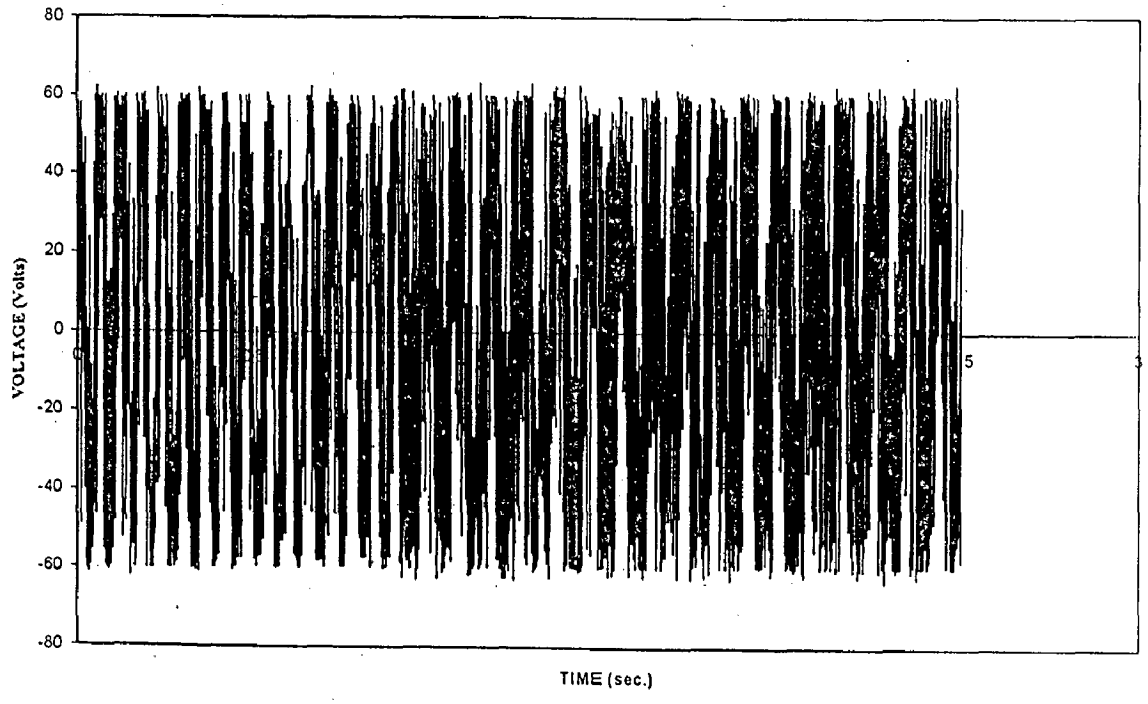

Fig.5.5(d) : STATOR PHASE VOLTAGE Vs TIME

CHAPTER -6

CONCLUSION

The control system design methodology and performance of permanent magnet synchronous motor drive is presented in this dissertation. This dissertation work investigates the speed control of a permanent magnet synchronous motor drive that is fed through a current hysteresis controlled PWM voltage source inverter. The main objective for using this controller is to minimize the deviation between the reference three phase line current commands and the feed back three phase line currents through the switching of inverter. The reference current commands are generated based on the principle that the resultant stator current vector is always kept in quadrature with the rotor flux vector. The goal is to achieve maximum generated torque per ampere during on-line operation.

The proportional integral controller is used as a speed controller to provide a fast speed response. For design of PI controller a mathematical model is developed from transfer function of different elements i.e., speed controller, permanent magnet synchronous motor. The speed controller has a transfer function, Kp + Ki/S. Its parameters Kp and Ki are found with the help of D-partition method.

To check the performance of permanent magnet synchronous motor drive, complete software is developed. The performance of the drive is investigated for change in reference speed and load variations.

It is evident from simulation studies that the current hysteresis controller provides one of the most effective methods for control of PMSM drive.

6.1 SCOPE FOR FUTURE WORK

Further work can be extended on the following points to get more detail of PMSM drive performance.

1. In present work PI controller has been used, but H^2 or H^∞ controller can be used for better results and more advanced motor controllers.
2. This technique can be implemented experimentally by using the software developed and experimental results can be compared.
3. In present work harmonics are neglected. The performance can be analyzed with harmonics.

REFERENCES

1. B.K. Bose, "Power Electronics and Variable Frequency Drives", IEEE Press 1996.
2. P. Pillay and R.Krishnan, "Modeling, Simulation, and Analysis of Permanent – Magnet Motor Drives, Part I: The Permanent-Magnet Synchronous Motor Drive", IEEE Transactions on Industry Applications, Vol.25, No.2, March/April 1989, pp. 265-273.
3. T.H.Liu and C.P.Cheng, "Controller Design for a Sensorless Permanent-Magnet Synchronous Drive System", IEE Proceedings-B, Vol.140, No.6, November 1993, pp. 369-378.
4. M.L. Mazenc, C.Villanueva and J.Hector, "Study and Implementation of Hysteresis Controlled Inverter on a Permanent Magnet Synchronous Machine", IEEE Transaction on Industry Applications, Vol. IA-21, No.2, March/April 1985, pp 408-413.
5. T.H.Liu, C.M.Young and C.H.Liu, "Microprocessor-Based Controller Design and Simulation for a Permanent Magnet Synchronous Motor Drive", IEEE Transaction on Industrial Electronics, Vol.35, No.4, November 1988, pp. 516-523.

6. D.M. Brod and D.W. Novothy, "Current Control of VSI-PWM Inverters", IEEE Transaction on Industry Applications, Vol.IA-21, No.4, May/June 1985, pp. 562-570.

7. Karl J.Strhat "Modern Permanent Magnets for Application in Electro-Technology" proceedings of the IEEE, Vol.78, No.6, June 1990, pp. 923-946.

8. M.A. Rahman and G.R.Slemon "Promising Applications of Neodymium Boron Iron magnets in Electrical Machines (invited)" IEEE Transactions. On Magnetics, Vol. MAG-21 No. 5 September 1985, pp 1712-1719.

9. Thomas M.Johns "Motion Control with Permanent Magnet AC Machines" proceedings of the IEEE, Vol.82, No.8, August 1994, pp. 1241-1252.

10. Thomas M.Johns, "Flux Weakening Regime Operation of an Interior PM Synchronous Motor Drive", IEEE Transactions on Industry Applications, Vol.23, No.4, July/Aug.1987, pp. 681-689.

11. Ashok B.Kulkarni and Mehradad Ehsani, "A Novel Position Sensor Elimination Technique for the Interior Permanent-Magnet Synchronous Motor Drives", IEEE Transactions. On Industry Applications, Vol.28, No.1, Jan/Feb.1992, pp. 144-150.

12. M.F. Rahman, L.Zhong and K.W.Lim, "A Direct Torque-controlled Interior PM Synchronous Motor Drive In Corporating Field

Weaksening", IEEE Transactions on Industry Applications, Vol.34, No.6, Nov./Dec.1998, pp. 1246-1253.

13. M.Bilewaski and others, "Control of High Performance Interior PM Synchronous Drives", IEEE Transactions on Industry Application, Vol.29, No.2, March/April 1993, pp. 328-336.

14. R.Krishnan and Shiyoung Lee, "PM Brushless DC motor Drive with New Power Converter Topology", IEEE Transactions on Industry Applications, Vol.33, No.4, 1997, pp.973-892.

15. M.J.Corley and R.D.Lorenz, "Rotor Position and Velocity Estimation for a Salient-pole PM Synchronous Machine at Stand-still and High speed", IEEE Transactions on Industry Applications Vol.34, No.4, July/Aug.1998, pp. 784-789.

16. R.B.Sepe and J.H.Lang, "Real-Time Adaptive Control of the Permanent Magnet Synchronous Motor", IEEE Transactions on Industry Applications, No.27, No.4, July/Aug.1991, pp. 706-714.

17. R.B.Sepe and J.H.Lang, "Real-Time Observe-Based (Adaptive) Control of a PM Synchronous Motor without Mechanical Sensors", IEEE Transactions On Industry Applications, Vol.28, No.6, Nov./Dec.1992, pp. 1345-1352.

18. Pragasen Pillay and Ramu Krishnan, "Application Characteristics of PM Synchronous and Brushless dc Motor for Servo Drives", IEEE Transactions on Industry Applications, Vol.27, No.5, Sept./Oct.1991, pp. 986-997.

19. C.C.Chan and others, "Novel PM motor drives of Electric Vehicles", IEEE Transactions on Industrial Electronics, Vol.43, No.2, April 1996, pp. 331-339.

20. T.J.E. Miller, "Brushless Permanent Magnet and Reluctance Motor Drives", Oxford Science Publications, Clarendon Press, Oxford, 1989.

APPENDIX – A

METHOD OF STABILITY ANALYSIS

For the stability analysis of linearised system and for parametric coordination, the D-partition method has been used in the present work. This method is capable of analysing any two parameters involved in any two of the coefficients of the characteristic equation. It gives a boundary between possible stable and unstable zone in parametric plane. A point check to confirm stability is then made with frequency scanning method.

In the present work, this method is used to design the parameters of speed controller used in the system. The transient responses for the small disturbances are obtained to select the best values of parameters to give better stability as well as fast transient response.

A.1 D-Partition Method

This method is also known as D-decomposition method. The method provides a means for determining the region of stability in the plane of a specified parameter or two parameters. In the present work the stability boundary has been plotted in the plane of two parameters at a time. This region of stability is also known are Vishnegradskii diagram. The Vishnegradiskii diagram may thus be obtained by constructing the D-

partition of the plane of the two real parameters, i.e. the plane section of the D-partition of the parameter space.

Let us suppose that the coefficients of the characteristic equation of the system.

$a_o p^n + a_1 p^{n-1} + a_2 p^{n-2} + \ldots\ldots\ldots\ldots + a_n = 0$

Depend on two parameters K_1 and K_2 and let us restrict ourselves to the case when these parameters enter into the equation linearly so that this equation can be reduced to the form

$$K_1 S(p) + K_2 Q(p) + R(p) = 0$$

Putting further $p = jw$ and separating real and imaginary parts, we obtain

$$K_1 S(jw) + K_2 Q(jw) + R(jw) = v(w) + ju(w) = 0$$

In the general case both function u(w) and v(w) depend not only on, but also on the two parameters K_1 and K_2. In order to construct the boundary of the D-partition it is necessary to determine K_1 and K_2 for each w, by solving simultaneously the two equations.

$$u(w) = 0 \text{ and } v(w) = 0$$

If in each of them we separate the terms containing K_1 and K_2 then a set of two equations with two unknowns are obtained as follows.

$$u(w) = K_1 S_1(w) + K_2 Q_1(w) + R_1(w) = 0$$

$$v(w) = K_1 S_2(w) + K_2 Q_2(w) + R_2(w) = 0$$

Solving this set of two linear algebraic equations with respect to K_1 and K_2 for each value of w we obtain,

$$K_1 = \frac{\begin{vmatrix} -R_1 & Q1 \\ -R_2 & Q_2 \end{vmatrix}}{\begin{vmatrix} S_1 & Q_1 \\ S_2 & Q_2 \end{vmatrix}} = \frac{-R_1Q_2 + R_2Q_2}{S_1Q_2 - S_2Q_1}$$

$$K_2 = \frac{\begin{vmatrix} S_1 & R1 \\ S_2 & R_2 \end{vmatrix}}{\begin{vmatrix} S_1 & Q_1 \\ S_2 & Q_2 \end{vmatrix}} = \frac{-S_1R_2 + S_2R_1}{S_1Q_2 - S_2Q_1}$$

The equation determine one value of K_1 and K_2 for each w only when these equations are simultaneous and independent. If for some value of w the numerator and denominator of above equations u(w) = 0 or v(w) = 0 is a consequence of the other, and for this value of w not a point but a straight line in the plane of K_1 and K_2 is obtained. In this case, either of the equation u(w) = 0 or v(w) = 0 is the equation of straight line when this value of w is substituted.

If the coefficient of the highest term of the characteristic equation depends on the parameters K_1 and K_2, then , by equating this coefficient to zero, the equation of another straight line corresponding to $w = \infty$ is obtained. These straight lines are called singular special lines.

In order to shade the boundary of the D-partition boundary one must move along the boundary in the direction of w increasing, and shade it on the left side if those points for which D>0 and on the right side for those points for which D<0

$$\text{where } D = \begin{vmatrix} S_1 & Q_1 \\ S_2 & Q_2 \end{vmatrix}$$

Usually this curve is traversed twice: once when w goes from - ∞ to 0, and then when it changes from 0 to ∞ , but it is shaded both times on the same side, since usually the sign of D changes for w> 0 and w< 0. Near the point of intersection of the curve and the straight line (w being same at intersection) their shaded sides must be directed towards one another.

The possible stable zone is determined as the inner most region in the sense of shading. To ensure that the possible stable zone is a stable zone, a point check for stability in the zone may be done by the Frequency scanning technique.

A. 2 Frequency Scanning Technique (Mikhailov Criterion)

Let D (p) = 0

be the characteristic equation of the system, where D (p) may be a polynomial in p or may include hyperbolic functions of p. The method consists of finding a frequency w

Solving this set of two linear algebraic equations with respect to K_1 and K_2 for each value of w we obtain,

$$K_1 = \frac{\begin{vmatrix} -R_1 & Q1 \\ -R_2 & Q_2 \end{vmatrix}}{\begin{vmatrix} S_1 & Q1 \\ S_2 & Q_2 \end{vmatrix}} = \frac{-R_1Q_2 + R_2Q_2}{S_1Q_2 - S_2Q_1}$$

$$K_2 = \frac{\begin{vmatrix} S_1 & R1 \\ S_2 & R_2 \end{vmatrix}}{\begin{vmatrix} S_1 & Q_1 \\ S_2 & Q_2 \end{vmatrix}} = \frac{-S_1R_2 + S_2R_1}{S_1Q_2 - S_2Q_1}$$

The equation determine one value of K_1 and K_2 for each w only when these equations are simultaneous and independent. If for some value of w the numerator and denominator of above equations u(w) = 0 or v(w) = 0 is a consequence of the other, and for this value of w not a point but a straight line in the plane of K_1 and K_2 is obtained. In this case, either of the equation u(w) = 0 or v(w) = 0 is the equation of straight line when this value of w is substituted.

If the coefficient of the highest term of the characteristic equation depends on the parameters K_1 and K_2, then , by equating this coefficient to zero, the equation of another straight line corresponding to $w = \infty$ is obtained. These straight lines are called singular special lines.

In order to shade the boundary of the D-partition boundary one must move along the boundary in the direction of w increasing, and shade it on the left side if those points for which D>0 and on the right side for those points for which D<0

$$\text{where } D = \begin{vmatrix} S_1 & Q_1 \\ S_2 & Q_2 \end{vmatrix}$$

Usually this curve is traversed twice: once when w goes from - ∞ to 0, and then when it changes from 0 to ∞ , but it is shaded both times on the same side, since usually the sign of D changes for w> 0 and w< 0. Near the point of intersection of the curve and the straight line (w being same at intersection) their shaded sides must be directed towards one another.

The possible stable zone is determined as the inner most region in the sense of shading. To ensure that the possible stable zone is a stable zone, a point check for stability in the zone may be done by the Frequency scanning technique.

A. 2 Frequency Scanning Technique (Mikhailov Criterion)

Let D (p) = 0

be the characteristic equation of the system, where D (p) may be a polynomial in p or may include hyperbolic functions of p. The method consists of finding a frequency w

(p= jw), where system parameters would satisfy the above equation. Frequency trajectories which are the result of plotting the imaginary part of D(jw) against its real part as frequency is varied from zero to infinity, are drawn. The frequency trajectory along with mirror image is shaded on the left side for $w = -\infty$ to $w = \infty$. If the origin is contained in the inner-most region (in the sense of shading) the system is stable

APPENDIX – B

The permanent Magnet Synchronous Motor selected for simulations has specifications as follows [5]

Electro-craft BLM – 2004 PMSM

Voltage	:	70 V
Power	:	600 W
Phase	:	3 (Star Connected)
L_d	:	4.04 mH
L_q	:	4.04 mH
r_1	:	0.31 Ω
J_m	:	0.00052 N-m Sec^2
$L_{md}\, i_{fd}$	:	0.384 N-m/A
Number of poles	:	4